Advances in Space Research

3D triangulation of Transient Luminous Events over Africa

--Manuscript Draft--

Manuscript Number:	AISR-D-22-00321R3
Article Type:	SI: Space/Geophys. on Africa
Keywords:	Transient Luminous Events triangulation; lightning peak current; lightning electric field
Corresponding Author:	Dakalo Casca Mashao University of Kwazulu-Natal Durban, KwaZulu Natal SOUTH AFRICA
First Author:	Dakalo Casca Mashao
Order of Authors:	Dakalo Casca Mashao
	Michael Jurgen Kosch
	Martin Fullekrug
	Nickolay Ivchenko
Abstract:	We present the first 3D triangulation of Transient Luminous Events (TLEs) over Africa. The 6 TLEs were simultaneously observed in the middle atmosphere from Sutherland and Carnarvon in South Africa, separated by 192 km, during the 2019 sprites campaign. These two distinctive locations have low radio interference and are free from light pollution. The lightning times, locations, peak current, and polarities, which initiated the observed TLEs, were obtained from the South African Lightning Detection Network and Earth Networks Total Lightning Networks. We investigate the TLEs' altitude and horizontal displacement from their parent lightning strokes. TLEs appear approximately 12.5 to 49.3 km away from their parent lightning strokes. We found that TLE altitudes range from 29 to 92.6 km. The lightning electric field and peak current may be related to the displacement of TLEs and the TLEs' horizontal spread.

No interests to declare

Transient Luminous Events 3D triangulation over Africa

D. Mashao[(1, 2)], M. Kosch[(1, 2,3,4)], M. Fullekrug[(5)], and M. Ivchenko[(6)]

[1]Department of Physics, University of KwaZulu-Natal, Durban, South Africa

[2]South African National Space Agency, Hermanus, South Africa

[3]Department of Physics, Lancaster University, UK

[4]Department of Physics, University of Western Cape, Bellville, South Africa

[5]Department of Electronic and Electrical Engineering, University of Bath, Bath, UK

[6]KTH Royal Institute of Technology. Stockholm. Sweden

Abstract

We present the first 3D triangulation of Transient Luminous Events (TLEs) over Africa. The 6 TLEs were simultaneously observed in the middle atmosphere from Sutherland and Carnarvon in South Africa, separated by 192 km, during the 2019 sprites campaign. These two distinctive locations have low radio interference and are free from light pollution. The lightning times, locations, peak current, and polarities, which initiated the observed TLEs, were obtained from the South African Lightning Detection Network and Earth Networks Total Lightning Networks. We investigate the TLEs' altitude and horizontal displacement from their parent lightning strokes. TLEs tend to appear approximately 12.5 to 49.3 km away from their parent lightning strokes. We found that TLEs' altitudes range from 29 to 92.6 km. The lightning electric field and peak current may be related to the displacement of TLEs and the TLEs' horizontal spread.

Key words: sprites altitude, lightning, sprites displacement, Transient Luminous Events, gigantic jet.

Corresponding author: Dakalo Mashao (mashaodakalo@gmail.com, +277614725002)

1. Introduction

Sprites are very brief optical illuminations in the middle atmosphere at an altitude of about 40 to 90 km, mainly associated with positive cloud-to-ground (CG) lightning discharges and sometimes negative CGs (Boggs et al., 2015; Füllekrug et al., 2006; Lang et al., 2013; Liu et al., 2015; Lyons, 1996; Pasko et al., 2013; Siingh et al., 2012; Surkov and Hayakawa, 2020). However, there have been reports of sprites produced by inter or intracloud lightning (Neubert et al., 2005, 2008). TLEs such as sprites, elves, blue jets, gigantic jets, starters, and halos, are electrical optical discharge phenomena associated with lightning activities electric field above the thunderstorms at an altitude between about 15 to 100 km, above the Earth's ground (Liu et al., 2015; Pasko et al., 2013; Siingh et al., 2012; Surkov and Hayakawa, 2020). Sprites are the most common form of TLEs. Sprites may appear displaced away from their causal CG lightning locations. e.g., dancing sprites. Most sprites' altitude measurements have been done with the assumption that sprites are initiated over their parent lightning strokes, and sprites have been found to occur at an altitude ranging from about 45 to 95 km (Füllekrug et al., 2019; Li et al.,2012; Mashao et al., 2021; McHarg et al., 2007; Ren et al., 2021; Wescott et al., 1998). There have been reports on sprites' altitude triangulation (Sentman et al., 1995; Stenbaek-Nielsen et al., 2010; Soula et al., 2015; Wescott et al., 1998; Wescott et al., 2001), spanning from about 50 to 90 km (Sentman et al., 1995), 48 to 88 km (Wang et al., 2019), and up to 96 km (Stenbaek-Nielsen et al., 2010). Wescott et al. (1998) reported that the column sprites' top altitude ranged from 81.3 to 88.9 km. In 2001 Wescott et al. (2001) found that triangulation of sprite halos top altitude span from 73.5 to 85.3 km. Factors such as the number of stars visible, local clouds, viewing direction, angular resolution, atmospheric scattering, light pollution, camera gain setting, distance to sprite, and ambiguity in selecting sprites feature can affect sprites' altitude triangulation (Mlynarczyk et al., 2015).

The displacement between the sprites and their parent lightning strokes ranges from 8.2 to 49.6 km (Wang et al., 2019), 2.4 to 74.7 km (Bór et al., 2018), and 13 to 111 km (Lyons, 1996). Sao-Sabbas et al. (2003) found that most sprites events appeared within 50 km from their parent CG lightning flashes and the maximum displacement was approximately 82 km. According to Lu et al. (2013), sprites are displaced more than 30 km, and according to Mlynarczyk et al. (2015) sprites tend to displace up to 70 km from their parent lightning strokes. Füllekrug et al. (2001) triangulated sprites current and found that large spatial displacement of about 60 km, which corresponds to the azimuths of the sprite luminosity edges.

This paper presents the first altitude triangulation of TLEs and the horizontal displacement between TLEs and their parent lightning stroke locations observed over Africa. We also compare the lightning electric field strength measured by the extremely low frequency (ELF) receiver and lightning peak current from the lightning networks with TLEs optical recordings.

2. Observations

On 29 January 2019, 6 TLEs were simultaneously recorded from the South African Astronomical Observatory (SAAO) (32.38º S, 20.81º E) and Square Kilometre Array (SKA) (30.97º S, 21.98º E) in the Northern Cape, South Africa, see Figure 1. The TLEs occurred between 20:49:49 and 22:48:47 UTC. We were able to triangulate the altitude and location of only 6 TLEs due to poor geometry and the aforementioned mitigating factors above (Mlynarczyk et al., 2015).

Figure 1. Column sprites event observed a 20:49:49 UTC on the 29 January 2019 from SAAO (left) and SKA (right), Northern Cape, South Africa.

The triangulated TLEs were recorded using Watec 910Hx cameras with 8.0 mm f/1.4 C-mount lens, which provide a 29°/46.2° Vertical/Horizontal (V/H) Field of View (FOV), see

Figure 1. The Watec camera systems captured video frames at 25 fps, 40 ms frame period, 640×480 pixels, fixed gain, and 0.45 gamma factor, with 8-bit intensity resolution and 0.061°/0.072° V/H angular resolution.

2.1 TLEs triangulation

In order to perform successful TLEs' altitude and location triangulation, we fitted modeled stars onto the real stars on the background image of TLEs to determine the azimuth and elevation angle of each pixel on the TLE image. Assuming that the TLEs occurred above their parent lightning stoke locations, we estimated the altitude of the target TLE feature, by performing spherical and planar trigonometry in the horizontal plane and vertical planes, respectively. This technique is described in detail by Mashao et al. (2021). After the stars fitting, we used the cosine and sine rule of spherical trigonometry to obtain simultaneous solutions for the angle subtended to the great circle (A) and slant distance to TLEs (r), as presented in Eq. (1) and (2) below.

$$A = \sin^{-1}\left(\frac{-(2\times(h+R_E)\times(R_E\tan(\theta)))+\sqrt{(2\times(h+R_E)\times R_E\tan(\theta))^2-4\times\left(\frac{(h+R_E)^2}{(\cos(\theta))^2}\right)\times(R_E^2-(h+R_E)^2}}{2\times\left(\frac{(h+R_E)}{(\cos(\theta))^2}\right)}\right) \quad (1)$$

$$r = \frac{(h+R_E)\times\sin(A)}{\cos(\theta)} \quad (2)$$

Where A is the angle subtended by the great circle, h is the altitude, R_E is the Earth's radius, θ is the elevation angle from the camera sites to TLEs, and r is the slant distance to the TLEs.

Since we know the azimuth and elevation of every TLEs' image pixels and slant distance to TLEs, for a known altitude, we can convert local spherical coordinates to geographic coordinates to obtain two estimated coordinates (latitude, longitude) of the TLEs with respect to the two observation sites. Since we know the estimated TLEs' ground coordinates from each camera's location, we then used Google Earth Pro (version 7.3.4.8248) software to show the distance from the camera systems locations to the TLEs' estimated sites, see Figure 2. Figure 2 shows the TLEs' position triangulation. The position where the red lines intercept is the actual TLE's location on the ground. We then use the TLE's exact location to triangulate the altitude of the TLE. By iterating the TLEs' altitude, we resolve the apparent ambiguity between the TLE's position and altitude.

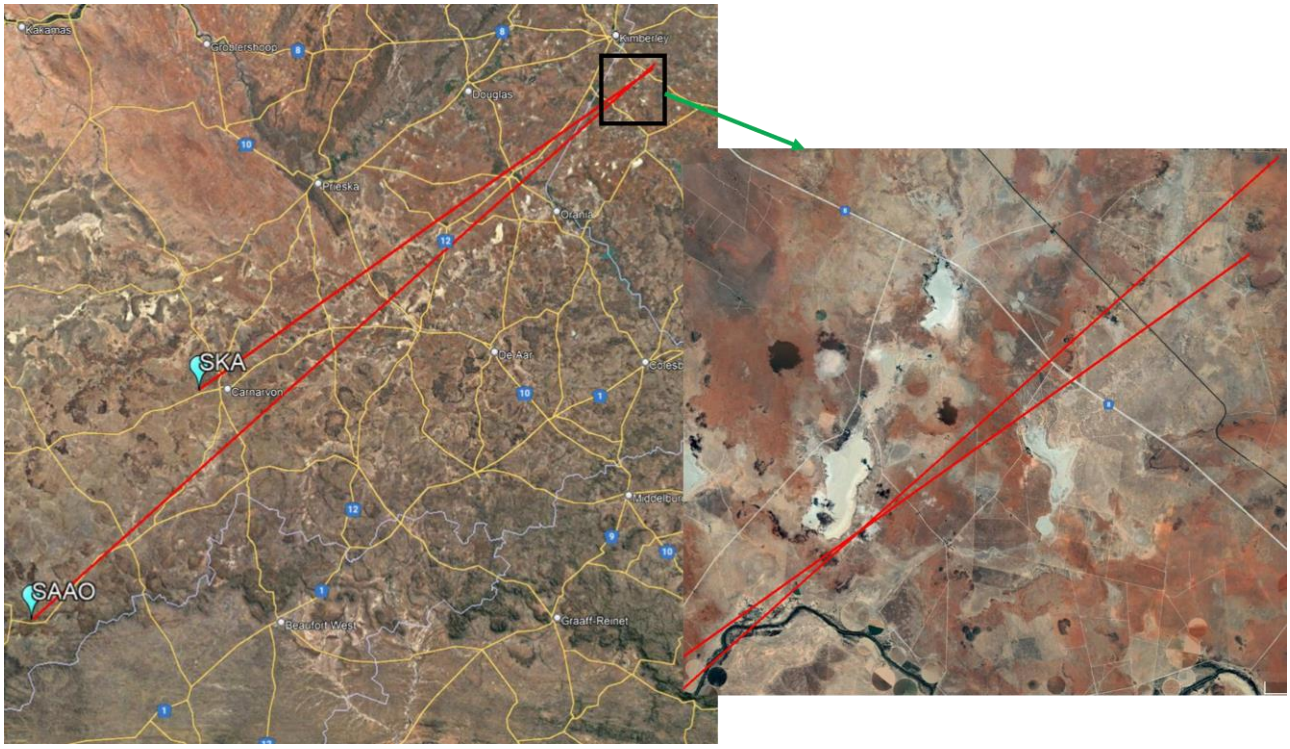

Figure 2. TLE location triangulation. The two turquoise symbols denote the locations of the cameras, which are SAAO and SKA. The red lines mark the distance from the camera locations to the estimated sprite locations. The position where the red lines intercept gives the actual TLE's location.

2.2 Lightning detection

The lightning location, time, and peak current information of the causal lightning stroke which generated the TLEs were provided by the South African Lightning Detection Networks (SALDN) and Earth Networks Total Lightning Networks (ENTLN). The SALDN operates 23 sensors with a 90% detection efficiency across South Africa. The SALDN ascertains the lightning locations, occurrence times, and polarities by acquiring the time of arrival and magnetic direction-finding methods. The ENTLN consists of 17 sensors over South Africa with a detection efficiency of approximately 60% to 70%. The ENTLN uses the time of arrival and sophisticated algorithms to determine lightning types, locations, time, and polarities. The SALDN and ENTLN have uncertainties in lightning locations of 0.5 km and 0.2 km, respectively (Gijben, 2012; Zhu et al., 2017). The distance to TLEs from SAAO and SKA were found to span from 511.7 to 590.1 km and 334.0 to 399.7 km, respectively. The parent lightning peak current varied from +23 to +92 kA.

The parent lightning vertical electric fields associated with the TLEs were recorded by a wideband ELF radio receiver in the frequency range ~4 Hz to 400 kHz. The ELF radio

receiver recorded the lighting vertical electric field with a sampling frequency of 1 MHz and 20 ns time accuracy. The lightning vertical electric field waveforms were used to determine the parent lightning electric field strength and the type of lightning associated with each TLE. The lightning electric field ranged from 1,101 to 1,570 mV/m at the receiver (Füllekrug, 2009; Füllekrug et al., 2019). The lightning electric field strength lessens with an increase in distance away from the lightning location. To compensate for this, we determine the electric field amplitude and the attenuation coefficient along the travelled path (Kolmašová et al., 2016). The electric field amplitude coefficient is determined by normalising the maximum lightning electric field strength at the receiver to 100 km from the lightning locations (Kolmašová et al., 2016). The experimental attenuation coefficient was found to be 0.41 dB/100 km. We found that the electric field amplitude at 100 km from the lightning locations spans 88.4 to 204 V/m, respectively.

All results are summarized in Table 1.

Table 1. Summary of TLEs triangulation observed on the 29 January 2019 as well as their parent lightning occurrence times, positions, and peak current provided by SALDN and ENTLN; lightning vertical electric field recorded by the ELF radio receiver; distance to sprites from SAAO and SKA; distance between TLE and lightning; TLEs' width and altitude of occurrence; and TLEs' morphological classification.

Time (UTC)	Lightning location (°)		TLEs location (°)		Distance from SAAO to TLEs (km)	Distance From SKA to TLEs (km)	Lightning peak current (kA)	Electric field at the receiver (mV/m)	Distance between TLE and lightning (km)	TLEs' maximum Horizontal size (km)	TLEs occurrence Altitude (km)	TLEs types
	LAT	LON	LAT	LON								
20:49:49.668	-29.23	24.79	-29.27	24.99	527.5	345.7	56	1,570	19.9	96.7	39.6—83.3	Column sprites
20:53:32.751	-28.96	24.73	-29.10	24.80	527.6	342	93	1,400	17	64.5	41—89.5	Jellyfish sprites
20:53:32.904	-29.22	24.79	-29.59	25.07	511	334.0	43	1,175	49.3	79.7	29—81	Gigantic jet
20:54:34.637	-30.19	25.53	-30.06	25.59	522.7	360.3	23	1,101	12.5	149.8	43.3—86.6	Column sprites (Halo)
21:05:51.251	-29.14	24.94	-28.99	24.94	545.6	360.1	92	1,247	16.7	116	43.5—92.6	Column sprites
22:48:06.932	-28.18	24.71	-28.30	24.75	590.1	399.7	44	1,230	13.9	66.7	47.7—82.6	Column sprites

3. Results and interpretation

3.1 TLEs altitude determination

Six TLEs were triangulated to simultaneously determine the actual TLEs' altitude and location. The six TLE events occurred in groups, and most of the TLEs were groups of column sprites. Two TLEs were classified as jellyfish sprites and gigantic jet (Surkov and Hayakawa, 2020). The distance from TLEs to SAAO and SKA varied from 511.7 to 590.1 km and 334 to 399.7 km, respectively. The lightning strokes that initiated the TLEs had peak current and electric field strength ranging from +23 to +92 kA and 1,101 to 1,570 mV/m at the receiver, respectively. The size of 6 TLEs spanned from 64.5 to 149.8 km horizontally. The triangulated TLEs' altitudes varied from 29 to 92.6 km, see Table 1. One TLE had a halo (see Table 1) of about 132 km diameter. The TLE, which had a bottom altitude of about 29 km, was classified as a gigantic jet (Surkov and Hayakawa, 2020). The TLEs' altitude difference between monostatic and triangulated estimates ranged from 1 to 2 km. For the monostatic method, the TLEs' altitudes were done with an assumption of TLEs occurring above the causal lightning stroke (Mashao et al., 2021). The uncertainty in altitude varied from ±0.33 to 0.47 km.

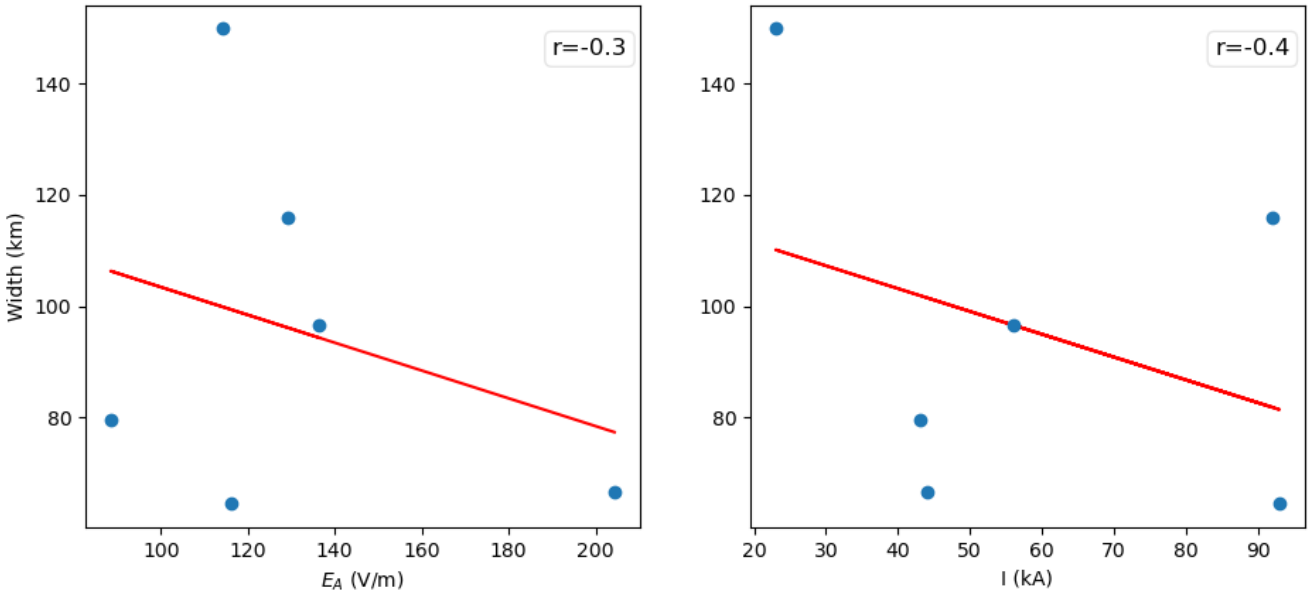

Figure 3. The relationship between the width of TLEs and the lightning electric field amplitude (E_A) at 100 km from their parent lightning locations (left) and peak current (I) (right), respectively. r shows the linear correlation coefficient.

Figure 3 shows the relationship between the width of TLEs and the lightning electric field amplitude (E_A) (left) at 100 km from their parent lightning locations and peak current (I) (right). A moderate linear correlation coefficient of -0.3 and -0.4 (Peat et al., 2009) was found between the width of TLEs and the lightning electric field amplitude and peak current, respectively. Although the data set is small, lightning electric field amplitude and peak current seem to be moderately related to TLEs' width.

3.2 TLEs position triangulation

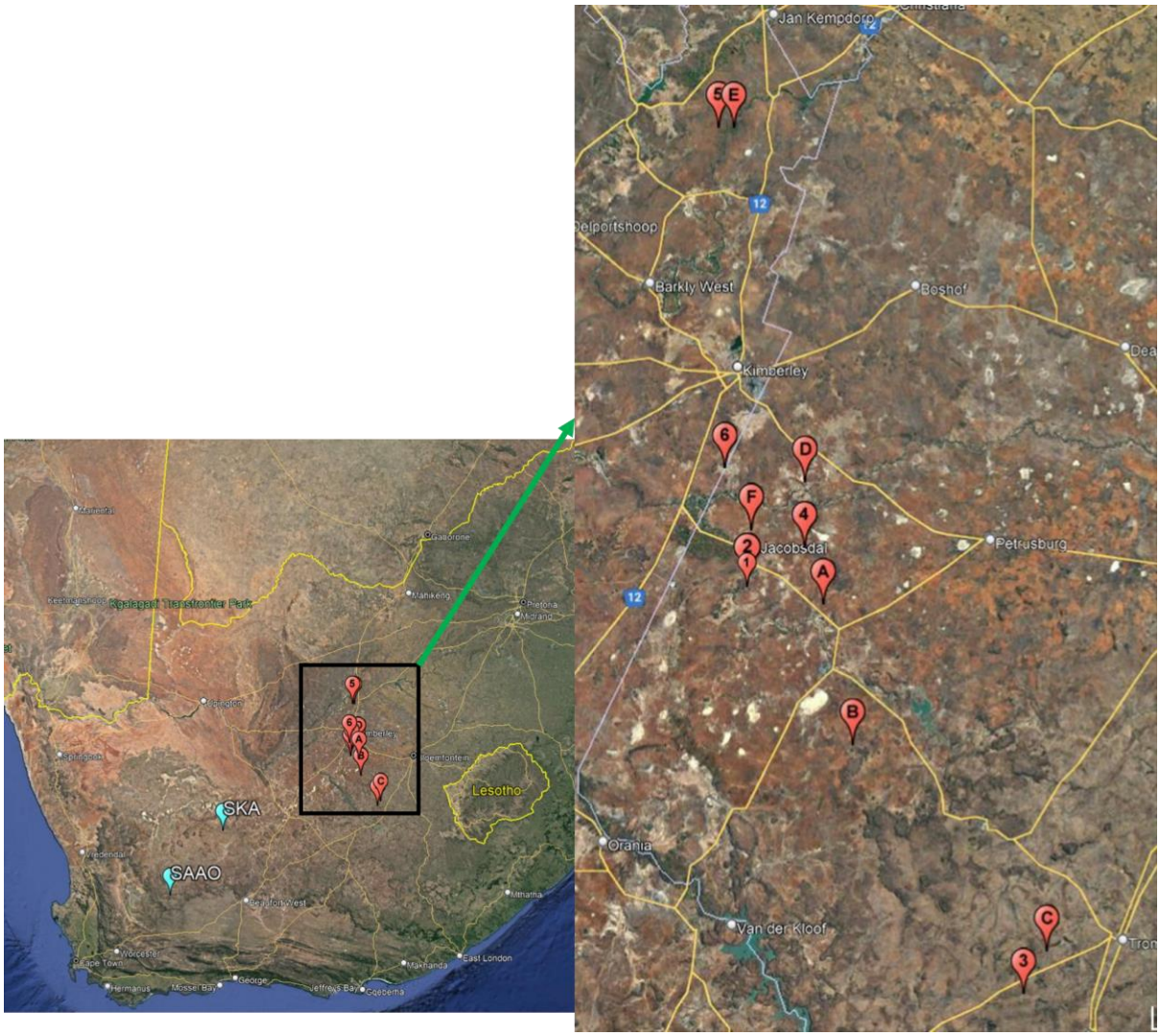

Figure 4. The locations of TLEs and their parent lightning strokes. The numbers and letters correspond to the position of parent lightning strokes and TLEs, respectively. E.g., lightning stroke 1, 2, 3, 4, 5, and 6 corresponds to TLE A, B, C, D, E, and F. SKA and SAAO mark the positions of cameras.

The displacement between 6 triangulated TLE features and their parent lightning stroke position were from 12.5 to 49.3 km. Our results agree with the results obtained elsewhere (Bór et al., 2018; Lu et al., 2013; Lyons, 1996; Mlynarczyk et al., 2015; Sao-Sabbas et al.,

2003; Wang et al., 2019). The uncertainty in position spanned from 0.2 km to 2 km. Figure 4 shows the TLEs' displacement from their parent lightning strokes.

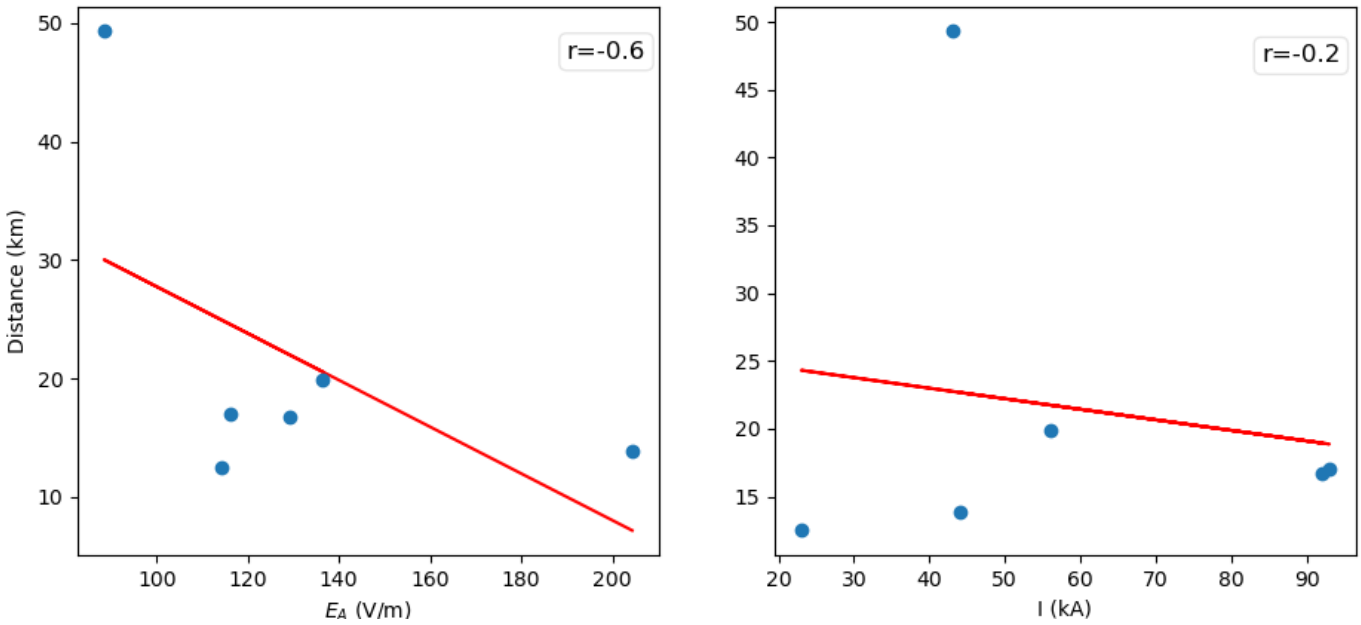

Figure 5. TLEs displayed distance from their parent lightning versus lightning electric field amplitude (E_A) at 100 km from their lightning locations (left) and peak current (I) (right), respectively. r shows the linear correlation coefficient.

The relationship between TLEs' displaced distance from their parent lightning and the lightning electric field amplitude (E_A) and peak current (I) is shown in Figure 5. A good and weak linear correlation coefficient of -0.6 and -0.2 (Peat et al., 2009) was found between the TLEs' displacement distance and lightning electric field amplitude and peak current, respectively. A large parent lightning electric field makes it more likely that the atmosphere overhead exhibits dielectric breakdown. Therefore, lightning discharges with large electric fields result in small TLE displacement away from their parent lightning strokes. We note the poor statistics.

4. Summary and Conclusions

We present the triangulation of six TLEs' positions on the Earth's surface and atmospheric altitudes. The CG lightning discharges associated with the TLEs have peak currents varying from +23 to +92 kA. The CG lightning electric field strength at the receiver and normalised to 100 km from their lightning stroke locations vary from 1,101 to 1,570 mV/m and 88.4 to 204 V/m, respectively. We found that the TLE displacement away from the lightning location spans from 12.5 to 49.3 km. The triangulated altitudes of the TLEs ranged from 29 to 92.6 km, and their width varied from 64.5 to 149.8 km. The TLEs' displacement away from their

parent lightning and TLE's width negatively correlates with their parent lightning normalised electric field amplitude. However, more data is required to confirm these results. The TLEs initiated by parent lightning with large electric field strength and peak current tend to display near their parent lightning location and with a less horizontal width.

5. Acknowledgments

This work was sponsored by the South African National Space Agency, University of KwaZulu-Natal, and the Royal Society (UK) grant NMG/R1/180252. DM, KM, and MF thanks the sponsors for their support.

6. References:

Boggs, L.D., Liu, N., Splitt, M., Lazarus, S., Glenn, C., Rassoul, H. and Cummer, S.A., 2016. An analysis of five negative sprite- parent discharges and their associated thunderstorm charge structures. *Journal of Geophysical Research: Atmospheres*, *121*(2), pp.759-784. https://doi.org/10.1002/2015JD024188

Bór, J., Zelkó, Z., Hegedüs, T., Jäger, Z., Mlynarczyk, J., Popek, M. and Betz, H.D., 2018. On the series of+ CG lightning strokes in dancing sprite events. *Journal of Geophysical Research: Atmospheres*, *123*(19), pp.11-030. https://doi.org/10.1029/2017JD028251

Füllekrug, M., Moudry, D.R., Dawes, G. and Sentman, D.D., 2001. Mesospheric sprite current triangulation. Journal of Geophysical Research: Atmospheres, 106(D17), pp.20189-20194. https://doi.org/10.1029/2001JD900075

Füllekrug, M., Mareev, E.A. and Rycroft, M.J. eds., 2006. *Sprites, elves and intense lightning discharges* (Vol. 225). Springer Science & Business Media. https://doi.org/10.1007/1-4020-4629-4

Füllekrug, M., 2009. Wideband digital low-frequency radio receiver. *Measurement Science and Technology*, *21*(1), p.015901. https://doi.org/10.1088/0957-0233/21/1/015901

Füllekrug, M., Nnadih, S., Soula, S., Mlynarczyk, J., Stock, M., Lapierre, J. and Kosch, M., 2019. Maximum sprite streamer luminosity near the Stratopause. *Geophysical Research Letters*, *46*(21), pp.12572-12579. https://doi.org/10.1029/2019GL084331

Gijben, M., 2012. The lightning climatology of South Africa. *South African Journal of Science*, *108*(3), pp.1-10. https://doi.org/10.4102/sajs.v108i3/4.740

Kolmašová, I., Santolík, O., Farges, T., Cummer, S.A., Lán, R. and Uhlíř, L., 2016. Subionospheric propagation and peak currents of preliminary breakdown pulses before negative cloud- to- ground lightning discharges. Geophysical Research Letters, 43(3), pp.1382-1391.

Lang, T.J., Cummer, S.A., Rutledge, S.A. and Lyons, W.A., 2013. The meteorology of negative cloud- to- ground lightning strokes with large charge moment changes: Implications for negative sprites. *Journal of Geophysical Research: Atmospheres*, *118*(14), pp.7886-7896. https://doi.org/10.1002/jgrd.50595

Li, J., Cummer, S., Lu, G. and Zigoneanu, L., 2012. Charge moment change and lightning-driven electric fields associated with negative sprites and halos. *Journal of Geophysical Research: Space Physics*, *117*(A9). https://doi.org/10.1029/2012JA017731

Liu, N., McHarg, M.G. and Stenbaek-Nielsen, H.C., 2015. High-altitude electrical discharges associated with thunderstorms and lightning. *Journal of Atmospheric and Solar-Terrestrial Physics*, *136*, pp.98-118. https://doi.org/10.1016/j.jastp.2015.05.013

Lu, G., Cummer, S.A., Li, J., Zigoneanu, L., Lyons, W.A., Stanley, M.A., Rison, W., Krehbiel, P.R., Edens, H.E., Thomas, R.J. and Beasley, W.H., 2013. Coordinated observations of sprites and in- cloud lightning flash structure. *Journal of Geophysical Research: Atmospheres*, *118*(12), pp.6607-6632. https://doi.org/10.1002/jgrd.50459

Lyons, W.A., 1996. Sprite observations above the US High Plains in relation to their parent thunderstorm systems. *Journal of Geophysical Research: Atmospheres*, *101*(D23), pp.29641-29652. https://doi.org/10.1029/96JD01866

Mashao, D.C., Kosch, M.J., Bór, J. and Nnadih, S., 2021. The altitude of sprites observed over South Africa. *South African Journal of Science*, *117*(1-2), pp.1-8. https://doi.org/10.17159/sajs.2021/7941

McHarg, M.G., Stenbaek- Nielsen, H.C. and Kammae, T., 2007. Observations of streamer formation in sprites. *Geophysical Research Letters*, *34*(6). https://doi.org/10.1029/2006GL027854

Mlynarczyk, J., Bór, J., Kulak, A., Popek, M. and Kubisz, J., 2015. An unusual sequence of sprites followed by a secondary TLE: An analysis of ELF radio measurements and optical

observations. *Journal of Geophysical Research: Space Physics*, *120*(3), pp.2241-2254. https://doi.org/10.1002/2014ja020780

Neubert, T., Allin, T.H., Blanc, E., Farges, T., Haldoupis, C., Mika, A., Soula, S., Knutsson, L., Van der Velde, O., Marshall, R.A. and Inan, U., 2005. Coordinated observations of transient luminous events during the EuroSprite2003 campaign. *Journal of Atmospheric and Solar-Terrestrial Physics*, *67*(8-9), pp.807-820. https://doi.org/10.1016/j.jastp.2005.02.004

Neubert, T., Rycroft, M., Farges, T., Blanc, E., Chanrion, O., Arnone, E., Odzimek, A., Arnold, N., Enell, C.F., Turunen, E. and Bösinger, T., 2008. Recent results from studies of electric discharges in the mesosphere. *Surveys in geophysics*, *29*(2), pp.71-137. https://doi.org/10.1007/s10712-008-9043-1

Peat, J., Barton, B. and Elliott, E., 2009. *Statistics workbook for evidence-based health care*. John Wiley & Sons. https://doi.org/10.1002/9781444300499

Pasko, V.P., Qin, J. and Celestin, S., 2013. Toward better understanding of sprite streamers: initiation, morphology, and polarity asymmetry. *Surveys in Geophysics*, *34*(6), pp.797-830. https://doi.org/10.1007/s10712-013-9246-y

Ren, H., Lu, G., Cummer, S.A., Peng, K.M., Lyons, W.A., Liu, F., Li, X., Wang, Y., Zhang, S. and Cheng, Z., 2021. Comparison between high- speed video observation of sprites and broadband sferic measurements. *Geophysical Research Letters*, *48*(10), p.e2021GL093094. https://doi.org/10.1029/2021GL093094

São Sabbas, F.T., Sentman, D.D., Wescott, E.M., Pinto Jr, O., Mendes Jr, O. and Taylor, M.J., 2003. Statistical analysis of space–time relationships between sprites and lightning. *Journal of Atmospheric and Solar-Terrestrial Physics*, *65*(5), pp.525-535. https://doi.org/10.1016/S1364-6826(02)00326-7

Sentman, D., Wescott, E., Osborne, D., Hampton, D. and Heavner, M., 1995. Preliminary results from the Sprites94 Aircraft Campaign: 1. Red sprites. *Geophysical Research Letters*, 22(10), pp.1205-1208. https://doi.org/10.1029/95GL00583

Soula, S., Defer, E., Füllekrug, M., Van Der Velde, O., Montanya, J., Bousquet, O., Mlynarczyk, J., Coquillat, S., Pinty, J.P., Rison, W. and Krehbiel, P.R., 2015. Time and space correlation between sprites and their parent lightning flashes for a thunderstorm observed

during the HyMeX campaign. Journal of Geophysical Research: Atmospheres, 120(22), pp.11-552. https://doi:10.1002/2015JD023894.

Stenbaek- Nielsen, H.C., Haaland, R., McHarg, M.G., Hensley, B.A. and Kanmae, T., 2010. Sprite initiation altitude measured by triangulation. *Journal of Geophysical Research: Space Physics*, *115*(A3). https://doi.org/10.1029/2009ja014543

Siingh, D., Singh, R.P., Singh, A.K., Kumar, S., Kulkarni, M.N. and Singh, A.K., 2012. Discharges in the stratosphere and mesosphere. *Space science reviews*, *169*(1-4), pp.73-121. https://doi.org/10.1007/s11214-012-9906-0

Surkov, V.V. and Hayakawa, M., 2020. Progress in the study of transient luminous and atmospheric events: a review. *Surveys in Geophysics*, *41*, pp.1101-1142. https://doi.org/10.1007/s10712-020-09597-2

Wang, Y., Lu, G., Ma, M., Zhang, H., Fan, Y., Liu, G., Wan, Z., Wang, Y., Peng, K.M., Peng, C. and Liu, F., 2019. Triangulation of red sprites observed above a mesoscale convective system in North China. Earth and Planetary Physics, 3(2), pp.111-125. https://doi: 10.26464/epp2019015

Wescott, E.M., Sentman, D.D., Heavner, M.J., Hampton, D.L., Lyons, W.A. and Nelson, T., 1998. Observations of 'Columniform'sprites. *Journal of atmospheric and solar-terrestrial physics*, *60*(7-9), pp.733-740. https://doi.org/10.1016/s1364-6826(98)00029-7

Wescott, E.M., Stenbaek- Nielsen, H.C., Sentman, D.D., Heavner, M.J., Moudry, D.R. and Sabbas, F.S., 2001. Triangulation of sprites, associated halos and their possible relation to causative lightning and micrometeors. *Journal of Geophysical Research: Space Physics*, *106*(A6), pp.10467-10477. https://doi.org/10.1029/2000ja000182

Zhu, Y., Rakov, V.A., Tran, M.D., Stock, M.G., Heckman, S., Liu, C., Sloop, C.D., Jordan, D.M., Uman, M.A., Caicedo, J.A. and Kotovsky, D.A., 2017. Evaluation of ENTLN performance characteristics based on the ground truth natural and rocket- triggered lightning data acquired in Florida. *Journal of Geophysical Research: Atmospheres*, *122*(18), pp.9858-9866. https://doi.org/10.1002/2017JD027270

To the Reviewers,

Thank you so much for the fruitful response. We have revised the manuscript accordingly. Please see our comments and responses below in green. The major voluntary changes (new paragraphs and whole new sentences) are written in green text in the manuscript.

Reviewer #1: The paper reports the first triangulation observation of Transient Luminous Events (TLEs) over Africa. The totally six TLEs were simultaneously observed by two cameras in South Africa, separated by 192 km. The horizontal displacement from TLEs and parent cloud-to-ground (CG) strokes are determined and about 12.5 km~49.3 km. In addition, authors present that the lightning electric field and peak current may be related to the displacement and horizontal spread of TLEs, which has not been reported by previous researcher.

Remarks

1. Because the triangulation needs to use the morphological characteristics of TLEs, this paper should describe TLEs in more detail and clearly. These images of TLEs could be shown in this paper to have an overview of morphological features.

More details on TLEs have been added in the manuscript on page 2, lines 33-57. The images of some of the TLEs we recorded are shown in Figure 1, page 4.

2. Line18-19: According to reported literature, GJs are usually preceded by intracloud lightning. Is there any evidence in this paper to show the correctness of its parent lightning?

We have clarified on the manuscript page 9, lines 202-208.

3. Please explain whether the time in Table 1 is the occurrence time of lightning or TLEs.

Occurrence time of lightning. Clarified in the manuscript on page 8, lines 183-184.

4. The key words given in the article are not accurate and should be considered.

New keywords are given in the manuscript on page 1, lines 22-23.

Reviewer #2:

Review of the manuscript entitled “Transient Luminous Events 3D triangulation over Africa”
by Mashao et al. submitted for a possible publication in Advances of Space Research [Manuscript ID: AISR-D-22-00321]
The manuscript present 3D triangulation of sprites observed over South Africa from two observation sites separated 192 km. Method of triangulation is described and sprite displacements from their parent lightning strokes are discussed. I believe that the study could be published in Advances in Space Research if the points made in the specific comments are addressed. I recommend a moderate revision.

Specific comments:
a) Equation (1), I believe there is a typo in Equation (1). The argument of sin-1 function should be unitless, [1]. However, it has the unit m.

We have rectified this in the manuscript on page 5, line 115.

b) The authors should discuss uncertainties of sprite localization. The cameras used certainly have an angular resolution (uncertainty) due to the limited number of pixels. This uncertainty will propagate, for example, into the uncertainty of the intercept, especially if the angle between the lines is as small as shown in Figure 2.

We have clarified this in the manuscript on page 11, lines 233-235.

c) I believe that the linear regression applied to the results shown in Figures 3 and 5 does not make sense. The data are widely scattered! For example, if we remove the point corresponding to a width of 149.8 km in Figure 3, which looks like an outlier, the regression line will be completely different. The same for plots and regression lines in Figure 5, if we remove the point corresponding to the distance 49.3 km, the regression line will be

completely different.

We have removed the linear regression in Figures 3 and 5.

d) I would also expect a discussion of whether the estimated attenuation coefficient is independent of the surrounding terrain and the bandwidth of the receiver used.

The discussion on the estimated attenuation coefficient is given in the manuscript on page 7, lines 159-165.

Thank you

3D triangulation of Transient Luminous Events over Africa

D. Mashao[(1, 2)], M. Kosch[(1, 2,3,4)], M. Fullekrug[(5)], and M. Ivchenko[(6)]

[1]Department of Physics, University of KwaZulu-Natal, Durban, South Africa

[2]South African National Space Agency, Hermanus, South Africa

[3]Department of Physics, Lancaster University, UK

[4]Department of Physics, University of Western Cape, Bellville, South Africa

[5]Department of Electronic and Electrical Engineering, University of Bath, Bath, UK

[6]KTH Royal Institute of Technology, Stockholm, Sweden

Abstract

We present the first 3D triangulation of Transient Luminous Events (TLEs) over Africa. The 6 TLEs were simultaneously observed in the middle atmosphere from Sutherland and Carnarvon in South Africa, separated by 192 km, during the 2019 sprites campaign. These two distinctive locations have low radio interference and are free from light pollution. The lightning times, locations, peak current, and polarities, which initiated the observed TLEs, were obtained from the South African Lightning Detection Network and Earth Networks Total Lightning Networks. We investigate the TLEs' altitude and horizontal displacement from their parent lightning strokes. TLEs appear approximately 12.5 to 49.3 km away from their parent lightning strokes. We found that TLE altitudes range from 29 to 92.6 km. The lightning electric field and peak current may be related to the displacement of TLEs and the TLEs' horizontal spread.

Keywords: Transient Luminous Events triangulation; lightning peak current; lightning electric field.

Corresponding author: Dakalo Mashao (mashaodakalo@gmail.com, +277614725002)

1. Introduction

TLEs such as sprites, elves, blue jets, gigantic jets, starters, and halos, are electrical optical discharge phenomena associated with the lightning activity electric field above thunderstorms at an altitude between about 15 to 100 km above the Earth's surface (Liu et al., 2015; Pasko et al., 2013; Siingh et al., 2012; Surkov and Hayakawa, 2020).

Blue jets, gigantic jets, and starters are connected with intracloud (IC) lightning activity, which involve the positive and negative charges of the thundercloud (Liu et al., 2015; Lu et al., 2011; Peng et al., 2018; Surkov and Hayakawa, 2020). They are generated above the thundercloud and move upwards to an altitude of about 40 to 50 km, 70 to 100 km, and 20 to 30 km, respectively. They have a duration vary from 417 to 650 ms, 60 to 90 ms, and 200 to 300 ms, respectively (Kuo et al., 2015; Liu et al., 2015; Peng et al., 2018; Rodger, 1999; Siingh et al., 2012; Surkov and Hayakawa, 2020).

Elves are a swelling thin ring induced by the electromagnetic pulse of either positive or negative cloud-to-ground (CG) lightning discharge at an altitude of about 85 to 95 km. Elves have a diameter of about 300 to 700 km and a duration of less than 1 ms (Frey et al., 2007; Liu et al., 2015; Williams et al., 2012; Surkov and Hayakawa, 2020). Halos are a spreading diffused flash of light associated with either the positive or negative CG lightning quasi-static electric field at an altitude of about 70 to 90 km (Taylor et al., 2008). Halos have a diameter of about 40 to 89 km and a duration of about 1 ms. Halos are occasionally followed by the initiation of sprites (Frey et al., 2007; Siingh et al., 2012; Surkov and Hayakawa, 2020; Taylor et al., 2008; Williams et al., 2012).

Sprites are very brief optical illuminations about 1 to 10 ms duration in the middle atmosphere at an altitude of about 40 to 90 km, mainly associated with positive CG lightning discharges and sometimes negative CGs (Boggs et al., 2015; Füllekrug et al., 2006; Lang et al., 2013; Liu et al., 2015; Lyons, 1996; Pasko et al., 2013; Siingh et al., 2012; Surkov and Hayakawa, 2020). However, there have been reports of sprites produced by inter or intracloud lightning (Neubert et al., 2005, 2008).

Sprites are the most common form of TLEs. Sprites may appear displaced away from their causal CG lightning locations, e.g. dancing sprites. Most sprites altitude measurements have been done with the assumption that sprites are initiated over their parent lightning strokes, and sprites have been found to occur at an altitude ranging from about 45 to 95 km (Füllekrug et al., 2019; Li et al.,2012; Mashao et al., 2021; McHarg et al., 2007; Ren et al., 2021;

Wescott et al., 1998). There have been reports on sprites altitude triangulation (Sentman et al., 1995; Stenbaek-Nielsen et al., 2010; Soula et al., 2015; Wescott et al., 1998; Wescott et al., 2001), spanning from about 50 to 90 km (Sentman et al., 1995), 48 to 88 km (Wang et al., 2019) and up to 96 km (Stenbaek-Nielsen et al., 2010). Wescott et al. (1998) reported that the column sprites' top altitude ranged from 81.3 to 88.9 km. Wescott et al. (2001) found that triangulation of sprite halos top altitude span from 73.5 to 85.3 km. Factors such as the number of stars visible, local clouds, viewing direction, angular resolution, atmospheric scattering, light pollution, camera gain setting, distance to sprite, and ambiguity in selecting a sprites feature can affect sprites' altitude triangulation (Mlynarczyk et al., 2015).

The displacement between the sprites and their parent lightning strokes ranges from 8.2 to 49.6 km (Wang et al., 2019), 2.4 to 74.7 km (Bór et al., 2018), and 13 to 111 km (Lyons, 1996). Sao-Sabbas et al. (2003) found that most sprites events appeared within 50 km from their parent CG lightning flashes and the maximum displacement was approximately 82 km. According to Lu et al. (2013), sprites are displaced more than 30 km, and according to Mlynarczyk et al. (2015) sprites tend to displace up to 70 km from their parent lightning strokes. Füllekrug et al. (2001) triangulated the lightning current and found a spatial displacement of about 60 km, from the edge of the sprite.

This paper presents the first 3D triangulation of the altitude of TLEs and the horizontal displacement between TLEs and their parent lightning stroke locations observed over Africa. We also compare the lightning electric field strength measured by an extremely low frequency (ELF) receiver and lightning peak current from the lightning networks with the TLEs optical recordings.

2. Observations

On 29 January 2019, 6 TLEs were simultaneously recorded from the South African Astronomical Observatory (SAAO) (32.38º S, 20.81º E) and Square Kilometre Array (SKA) (30.97º S, 21.98º E) in the Northern Cape, South Africa, see Figure 1. The TLEs occurred between 20:49:49 and 22:48:47 UTC. We were able to 3D triangulate the altitude and location of only 6 TLEs due to poor geometry and the aforementioned mitigating factors (Mlynarczyk et al., 2015). Figure 1 shows some of the TLEs observed on 29 January 2019, Gigantic jet (top left) at 20:53:32 UTC, sprites halo (top right) at 20:54:34 UTC, and a column sprites event observed simultaneously at 20:49:49 UTC from SAAO (bottom left) and SKA (bottom right), Northern Cape, South Africa.

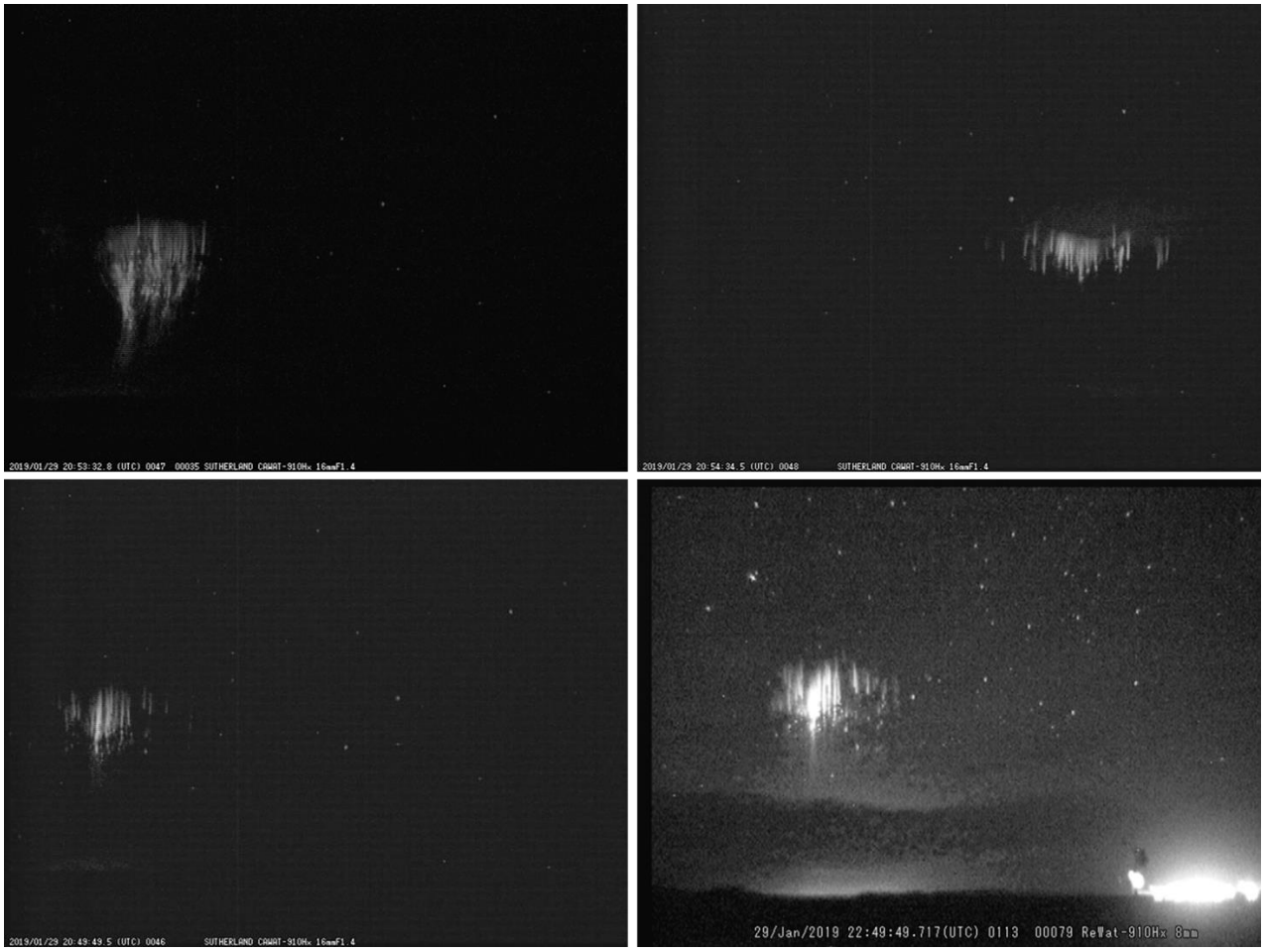

Figure 1. TLEs observed on 29 January 2019. Gigantic jet (top left) and sprites halo (top right) recorded at 20:53:32 and 20:54:34 UTC. Column sprites event observed a 20:49:49 UTC from SAAO (bottom left) and SKA (bottom right), Northern Cape, South Africa.

The triangulated TLEs were recorded using Watec 910Hx cameras with 8.0 mm f/1.4 C-mount lens, which provides a 29°/46.2° Vertical/Horizontal (V/H) Field of View (FOV), see Figure 1. The Watec camera systems captured video frames at 25 fps, 40 ms frame period, 640×480 pixels, fixed gain, and 0.45 gamma factor, with 8-bit intensity resolution and 0.061°/0.072° V/H pixel angular resolution.

2.1 TLEs triangulation

In order to perform successful TLEs altitude and location triangulation, we fitted modeled stars onto the real stars on the background image of TLEs to determine the azimuth and elevation angle of each pixel in the TLE image. Assuming that the TLEs occurred above their parent lightning stoke locations, we estimated the altitude of the target TLE feature, by performing spherical and planar trigonometry in the horizontal plane and vertical planes, respectively. This technique is described in detail by Mashao et al. (2021). After the stars

fitting, we used the cosine and sine rule of spherical trigonometry to obtain simultaneous solutions for the angle subtended on the great circle (A) and slant distance to TLEs (r), as presented in Eq. (1) and (2) below:

$$A = \sin^{-1}\left(\frac{-(2\times(h+R_E)\times(R_E\tan(\theta)))+\sqrt{(2\times(h+R_E)\times R_E\tan(\theta))^2-4\times\left(\frac{(h+R_E)^2}{(\cos(\theta))^2}\right)\times(R_E^2-(h+R_E)^2}}{2\times\left(\frac{(h+R_E)^2}{(\cos(\theta))^2}\right)}\right) \quad (1)$$

$$r = \frac{(h+R_E)\times\sin(A)}{\cos(\theta)} \quad (2)$$

where A is the angle subtended by the great circle, h is the altitude, R_E is the Earth's radius, θ is the elevation angle from the camera locations to the TLEs, and r is the slant distance to the TLEs.

Since we know the azimuth and elevation of every TLEs image pixels and slant distance to the TLEs, for a known altitude, we can convert local spherical coordinates to geographic coordinates to obtain two estimated coordinates (latitude, longitude) of the TLEs with respect to the two observation sites. Since we know the estimated TLEs ground coordinates from each camera's location, we then used Google Earth Pro (version 7.3.4.8248) software to show the distance from the camera systems locations to the TLEs estimated locations, see Figure 2. Figure 2 shows the TLEs position triangulation. The position where the red lines intercept is the actual TLE's location on the ground. We then use the TLE's exact location to adjust the altitude of the TLE by triangulation. By iteration, we resolve the apparent ambiguity between the TLE's geographic position and altitude.

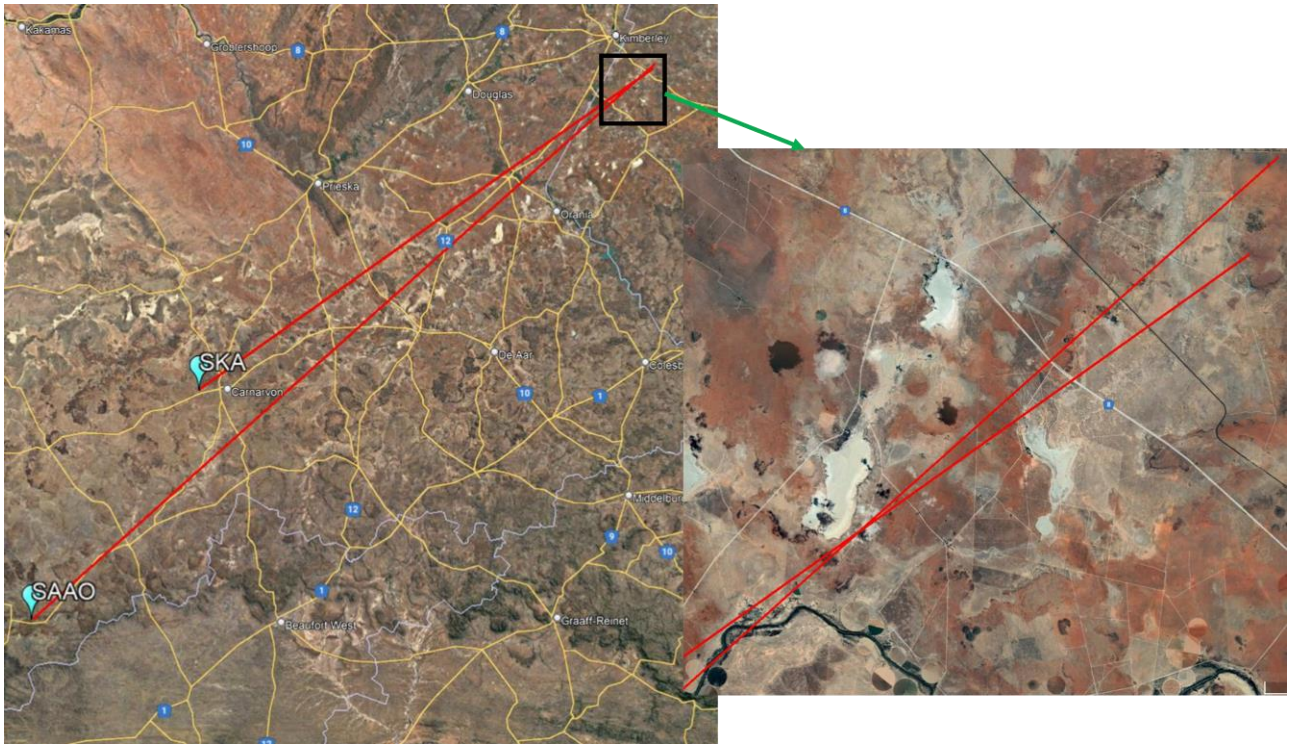

Figure 2. TLE location triangulation. The two turquoise symbols denote the locations of the cameras, which are SAAO and SKA. The red lines mark the distance from the camera locations to the estimated sprite location. The position where the red lines intercept gives the actual TLE's location.

2.2 Lightning detection

The lightning location, time, and peak current information of the causal lightning stroke which generated the TLEs were provided by the South African Lightning Detection Networks (SALDN) and Earth Networks Total Lightning Networks (ENTLN). The SALDN operates 23 sensors with a 90% detection efficiency across South Africa. The SALDN ascertains the lightning locations, occurrence times, and polarities by acquiring the time of arrival and magnetic direction-finding methods. The ENTLN consists of 17 sensors over South Africa with a detection efficiency of approximately 60% to 70%. The ENTLN uses the time of arrival and sophisticated algorithms to determine lightning types, locations, time, and polarities. The SALDN and ENTLN have uncertainties in lightning locations of 0.5 km and 0.2 km, respectively (Gijben, 2012; Zhu et al., 2017). The distance to TLEs from SAAO and SKA were found to span from 511.7 to 590.1 km and 334.0 to 399.7 km, respectively. The parent lightning peak current varied from +9 to +93 kA.

The parent lightning vertical electric fields associated with the TLEs were recorded by a wideband ELF radio receiver, located at SKA, in the frequency range ~4 Hz to 400 kHz. The

ELF radio receiver recorded the lighting vertical electric field with a sampling frequency of 1 MHz and 20 ns time accuracy. The lightning vertical electric field waveforms were used to determine the parent lightning electric field strength and the type of lightning associated with each TLE. The lightning electric field ranged from 204 to 1,570 mV/m at the receiver (Füllekrug, 2010; Füllekrug et al., 2019).

The lightning electric field strength lessens with an increase in distance away from the lightning location. To compensate for this, we determine the electric field amplitude and the attenuation coefficient along the travelled path (Kolmašová et al., 2016). The electric field amplitude coefficient is determined by normalising the maximum lightning electric field strength at the receiver to 100 km from the lightning locations (Kolmašová et al., 2016). We found an experimental attenuation coefficient of about 0.41 dB/100 km. The attenuation of a radio wave signal is low over the nighttime (Chapman and Macario, 1956), and our observations were made at nighttime within a low radio interference area, see Table 1. The attenuation coefficient depends on the bandwidth of the receiver, i.e. low frequency results in low attenuation. Kolmašová et al. (2016) used broadband with a bandwidth of 5 kHz – 37 MHz and obtained an attenuation coefficient of 2.15 dB/100 km (Kolmašová et al., 2016). We found that the electric field amplitude at 100 km from the lightning locations spanned 88.4 to 204 V/m, respectively. All results are summarized in Table 1.

Table 1. Summary of TLEs triangulation observed on the 29 January 2019 as well as their parent lightning occurrence times, positions, and peak current provided by SALDN and ENTLN; lightning vertical electric field recorded by the ELF radio receiver at SKA; distance to sprites from SAAO and SKA; distance between TLE and lightning; TLEs' width and altitude of occurrence; and TLEs' morphological classification. The times in the first column are the lightning occurrence times. +CG and +IC denote positive cloud to ground lightning stroke and positive Intracloud lightning discharge, respectively. The lightning discharge at 20:53:32.904 UTC and 20:53:33.013 UTC contributed to the generation of a gigantic jet. A, B, C, D, E, and F in column 11 (TLEs types) correspond to TLEs position in Figure 4.

Time (UTC)	Lightning location (°)		TLEs location (°)		Distance from SAAO to TLEs (km)	Distance From SKA to TLEs (km)	Lightning peak current (kA)	Electric field at the receiver (mV/m)	Distance between TLE and lightning (km)	TLE maximum Horizontal size (km)	TLEs triangulated Altitude (km)	TLEs types
	LAT	LON	LAT	LON								
20:49:49.668 (+CG)	-29.23	24.79	-29.27	24.99	527.5	345.7	56	1,570	19.9	96.7	39.6—83.3	Column sprites (A)
20:53:32.751 (+CG)	-28.96	24.73	-29.10	24.80	527.6	342	93	1,400	17	64.5	41—89.5	Jellyfish sprites (F)
20:53:32.904 (+CG)	-29.22	24.79	-29.59	25.07	511.7	334.0	43	1,175	49.3	79.7	29—81	Gigantic jet (B)
20:53:33.013 (+IC)	-29.23	24.81	-29.59	25.07			9	204	47.9			
20:54:34.637 (+CG)	-30.19	25.53	-30.06	25.59	522.7	360.3	23	1,101	12.5	149.8	43.3—86.6	Column sprites with (Halo) (C)
21:05:51.251 (+CG)	-29.14	24.94	-28.99	24.94	545.6	360.1	92	1,247	16.7	116	43.5—92.6	Column sprites (D)
22:48:06.932 (+CG)	-28.18	24.71	-28.30	24.75	590.1	399.7	44	1,230	13.9	66.7	47.7—82.6	Column sprites (E)

3. Results and interpretation

3.1 TLEs altitude determination

Six TLEs were triangulated to simultaneously determine the actual TLEs altitude and location. The six TLE events occurred in groups, and most of the TLEs were groups of column sprites. Two TLEs were classified as a jellyfish sprite and a gigantic jet (Surkov and Hayakawa, 2020). The distance from the TLEs to SAAO and SKA varied from 511.7 to 590.1 km and 334 to 399.7 km, respectively. The lightning strokes that initiated the TLEs had a peak current and electric field strength ranging from +23 to +93 kA and 1,101 to 1,570 mV/m at the receiver, respectively. The horizontal size of the 6 TLEs spanned from 64.5 to 149.8 km. The triangulated TLEs altitudes varied from 29 to 92.6 km, see Table 1. One TLE had a halo (see Table 1) of about 132 km diameter.

The TLE, which had a bottom altitude of about 29 km, was classified as a gigantic jet (Surkov and Hayakawa, 2020). The ENTLN reported an IC lightning discharge, which contributed to the initiation of the gigantic jet, 109 ms after the +CG lightning stroke located 1.7 km away from the +CG lightning stroke location. The +IC lightning discharge had a peak current and electric field of 9 kA and 204 mV/m at the receiver, respectively. The +IC lightning discharge was 47.9 km away from the gigantic jet. Thus, based on the locations and time of occurrence of the +CG and +IC lightning discharges, both lightning discharges contributed to the initiation of the gigantic jet.

The TLEs' altitude difference between monostatic and triangulated estimates ranged from 1 to 2 km. For the monostatic method, the TLE altitude estimates assumed that TLEs occurred above the causal lightning stroke (Mashao et al., 2021). The uncertainty in TLE altitude determined from the angular resolution of camera varied from ±0.33 to 0.47 km. The uncertainty depends on the slant distance to the TLE from the camera's location, which ranged from 336 to 600 km.

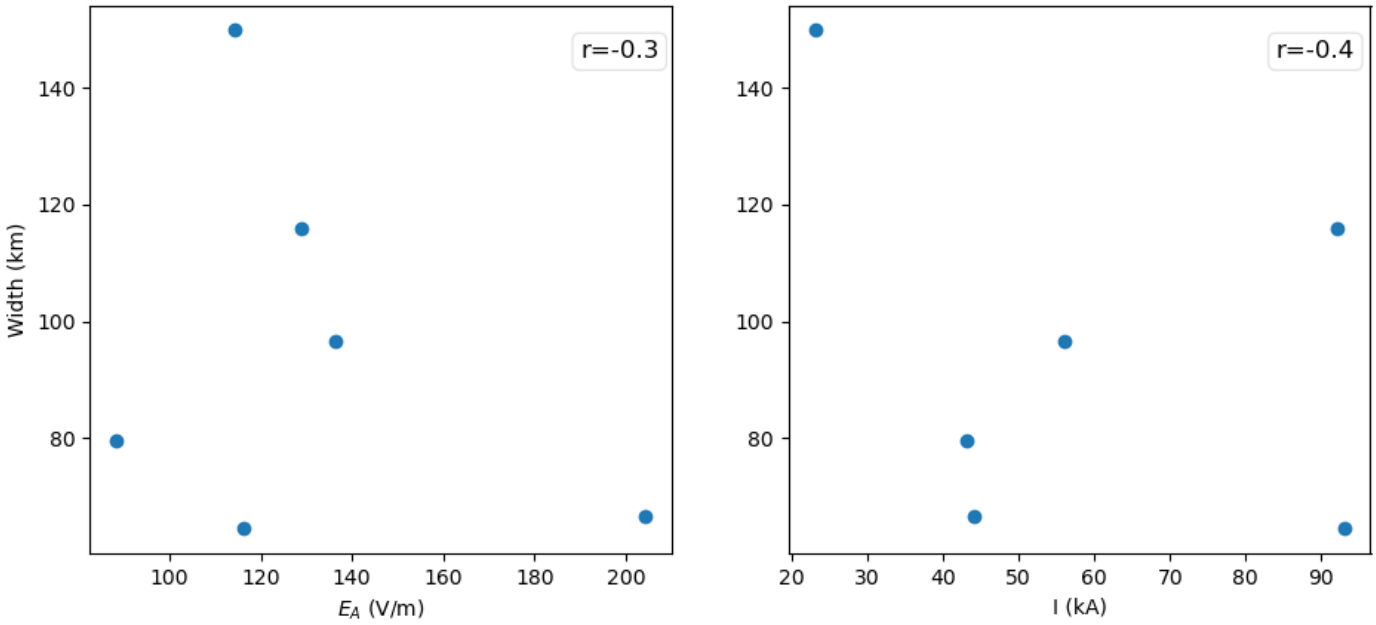

Figure 3. The relationship between the horizontal width of TLEs and the lightning electric field amplitude (E_A) at 100 km from their parent lightning locations (left) and peak current (I) (right), respectively. r shows the linear correlation coefficient.

Figure 3 shows the relationship between the horizontal width of the TLEs and the lightning electric field amplitude (E_A) (left) at 100 km from their parent lightning locations and peak current (I) (right). A moderate linear correlation coefficient of -0.3 and -0.4 (Peat et al., 2009) was found between the width of TLEs and the lightning electric field amplitude and peak current, respectively. Although the data set is small, lightning electric field amplitude and peak current seem to be moderately related to the TLEs width.

3.2 TLEs position triangulation

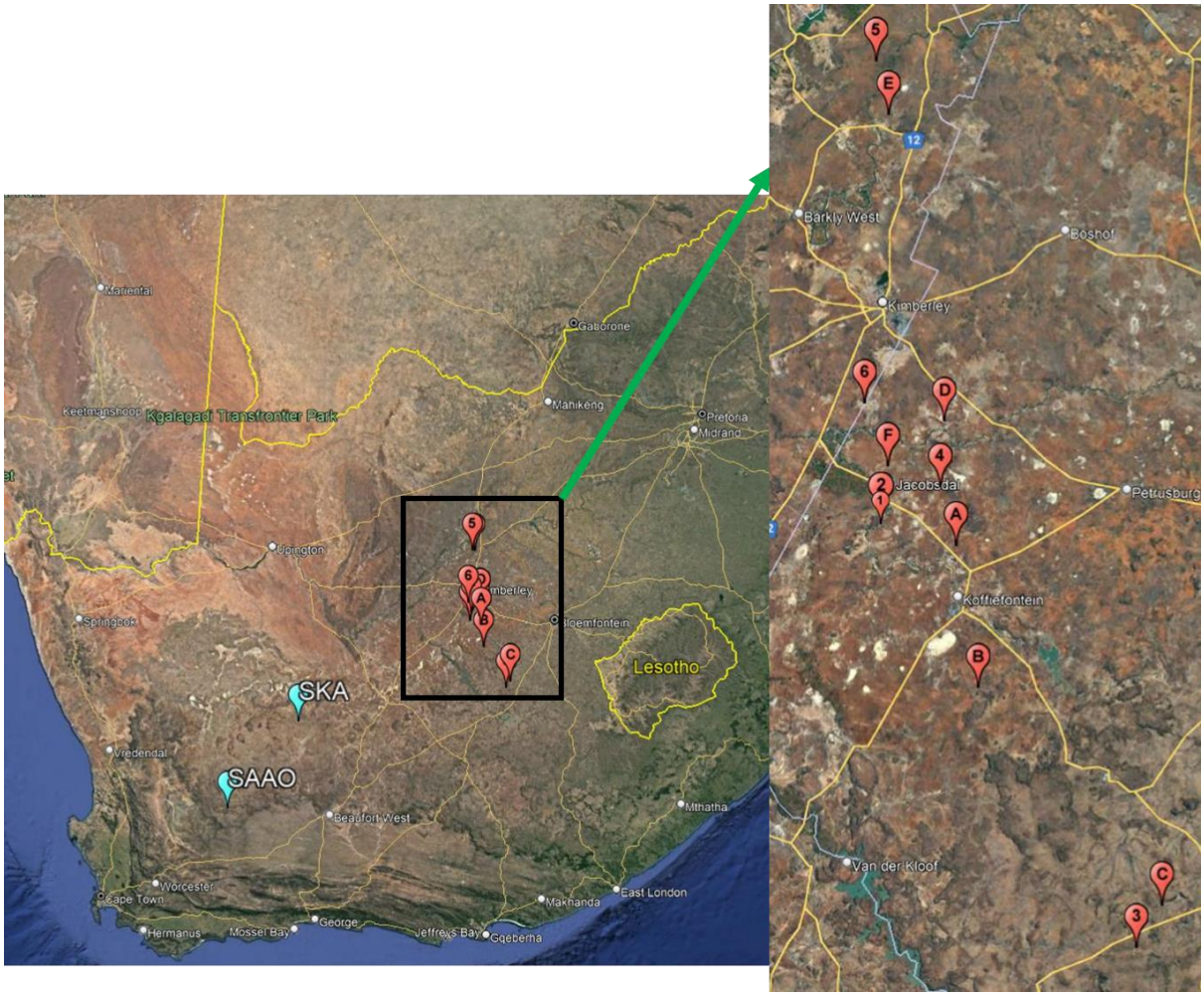

Figure 4. The locations of TLEs and their parent lightning strokes. The numbers and letters correspond to the position of parent lightning strokes and TLEs, respectively. E.g., lightning stroke 1, 2, 3, 4, 5, and 6 corresponds to TLE A, B, C, D, E, and F. SKA and SAAO mark the positions of the cameras.

The displacement between 6 triangulated TLE features and their parent lightning stroke position were from 12.5 to 49.3 km. Our results are in good agreement with similar results obtained elsewhere (Bór et al., 2018; Lu et al., 2013; Lyons, 1996; Mlynarczyk et al., 2015; Sao-Sabbas et al., 2003; Wang et al., 2019). The uncertainty in sprites geographic location, which depends on the angular resolution of the cameras and the viewing geometry to the TLEs, averaged 7.2 km with a standard deviation of 7.1 km. Figure 4 shows the TLEs' displacement from their parent lightning strokes.

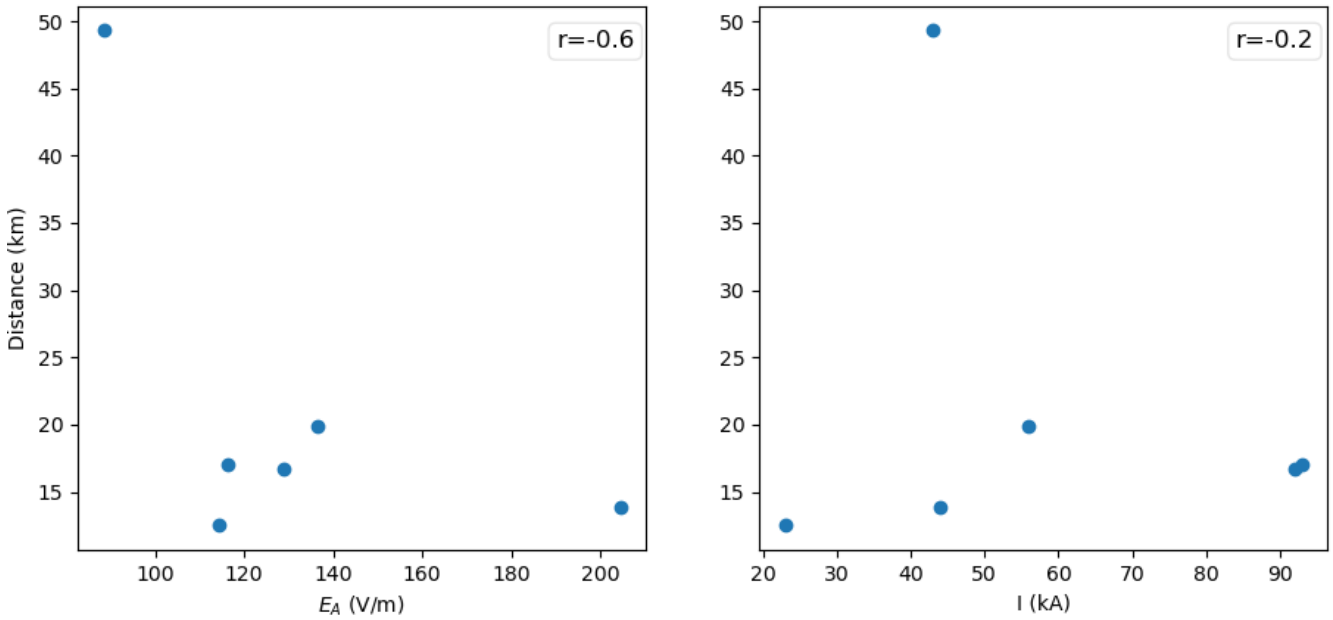

Figure 5. TLEs displayed distance from their parent lightning versus lightning electric field amplitude (E_A) at 100 km from their lightning locations (left) and peak current (I) (right), respectively. r shows the linear correlation coefficient.

The relationship between the TLEs' displaced distance from their parent lightning and the lightning electric field amplitude (E_A) and peak current (I) is shown in Figure 5. A good and weak linear anti-correlation coefficient of -0.6 and -0.2 (Peat et al., 2009) was found between the TLEs displacement distance and lightning electric field amplitude and peak current, respectively. A large parent lightning electric field makes it more likely that the atmosphere overhead exhibits dielectric breakdown. Therefore, lightning discharges with large electric fields result in a small TLE displacement away from their parent lightning stroke. We note the poor statistics.

4. Summary and Conclusions

We present the 3D triangulation of six TLEs positions on the Earth's surface and atmospheric altitudes. The CG lightning discharges associated with the TLEs have peak currents varying from +23 to +93 kA. The CG lightning electric field strength at the receiver and normalised to 100 km from their lightning stroke locations vary from 1,101 to 1,570 mV/m and 88.4 to 204 V/m, respectively. We found that the TLE displacement away from the lightning location spanned from 12.5 to 49.3 km. The triangulated altitudes of the TLEs ranged from 29 to 92.6 km, and their width varied from 64.5 to 149.8 km. The TLEs displacement away from their parent lightning and TLE width negatively correlates with their parent lightning normalised electric field amplitude. However, more data is required to confirm these results. The TLEs

initiated by parent lightning with a large electric field strength and peak current tend to display near their parent lightning location and with a less horizontal width.

5. Acknowledgments

This work was sponsored by the South African National Space Agency, University of KwaZulu-Natal, and the Royal Society (UK) grant NMG/R1/180252. DM, KM, and MF thank the sponsors for their support. The authors thank the South African Lightning Detection Networks and Earth Networks Total Lightning Networks for providing the lightning data.

6. References:

Boggs, L.D, Liu, N., Splitt, M et al., 2016. An analysis of five negative sprite- parent discharges and their associated thunderstorm charge structures. *J. Geophys. Res. Atmos*. *121*(2), 759-784. https://doi.org/10.1002/2015JD024188

Bór, J., Zelkó, Z., Hegedüs, T et al., 2018. On the series of+ CG lightning strokes in dancing sprite events. *J. Geophys. Res. Atmos*. *123*(19), 11-030. https://doi.org/10.1029/2017JD028251

Chapman, F.W. and Macario, R.C.V., 1956. Propagation of audio-frequency radio waves to great distances. *Nature*, *177*(4516), 930-933. https://doi.org/10.1038/177930a0

Frey, H.U., Mende, S.B., Cummer, S.A., et al., 2007. Halos generated by negative cloud-to- ground lightning. *Geophys. Res. Lett*. 34(18), L18801. https://doi.org/10.1029/2007gl030908

Füllekrug, M., Moudry, D.R., Dawes, G et al., 2001. Mesospheric sprite current triangulation. *J. Geophys. Res. Atmos. 106*(D17), 20189-20194. https://doi.org/10.1029/2001JD900075

Füllekrug, M., Mareev, E.A. Rycroft, M.J. eds., 2006. Sprites, Elves and intense Lightning Discharges (Vol. 225). *NATO Science Series II. Mathematics, physics and chemistry*, Dordrecht: *Springer*, ISBN 1-4020-4628-630-42, 30-32. https://doi.org/10.1007/1-4020-4629-4

Füllekrug, M., 2010. Wideband digital low-frequency radio receiver. *Meas. Sci. Technol. 21*(1), 1-9. https://doi.org/10.1088/0957-0233/21/1/015901

Füllekrug, M., Nnadih, S., Soula, S et al., 2019. Maximum sprite streamer luminosity near the Stratopause. *Geophys. Res. Lett*. *46*(21), 12572-12579. https://doi.org/10.1029/2019GL084331

Gijben, M., 2012. The lightning climatology of South Africa. *S. Afr. J. Sci*, *108*(3), 1-10. https://doi.org/10.4102/sajs.v108i3/4.740

Kolmašová, I., Santolík, O., Farges, T et al., 2016. Subionospheric propagation and peak currents of preliminary breakdown pulses before negative cloud- to- ground lightning discharges. *Geophys. Res. Lett. 43*(3), 1382-1391. https://doi:10.1002/2015GL067364.

Kuo, C.L., Su, H.T. and Hsu, R.R., 2015. The blue luminous events observed by ISUAL payload on board FORMOSAT- 2 satellite. *J. Geophys. Res. Space Phys. 120*(11), 9795-9804. https://doi.org/10.1002/2015JA021386

Lang, T.J., Cummer, S.A., Rutledge, S.A et al., 2013. The meteorology of negative cloud-to- ground lightning strokes with large charge moment changes: Implications for negative sprites. *J. Geophys. Res. Atmos. 118*(14), 7886-7896. https://doi.org/10.1002/jgrd.50595

Li, J., Cummer, S., Lu, G. et al., 2012. Charge moment change and lightning- driven electric fields associated with negative sprites and halos. *J. Geophys. Res. Space Phys*. *117*(A9), A09310. https://doi.org/10.1029/2012JA017731

Liu, N., McHarg, M.G. and Stenbaek-Nielsen, H.C., 2015. High-altitude electrical discharges associated with thunderstorms and lightning. *J. Atmos. Sol. Terr. Phys. 136*, 98-118. https://doi.org/10.1016/j.jastp.2015.05.013

Lu, G., Cummer, S.A., Lyons, W.A et al., 2011. Lightning development associated with two negative gigantic jets. *Geophy. Res. Lett. 38*(12), L12801. https://doi.org/10.1029/2011GL047662

Lu, G., Cummer, S.A., Li, J et al., 2013. Coordinated observations of sprites and in- cloud lightning flash structure. *J. Geophys. Res. Atmos. 118*(12), 6607-6632. https://doi.org/10.1002/jgrd.50459

Lyons, W.A., 1996. Sprite observations above the US High Plains in relation to their parent thunderstorm systems. *J. Geophys. Res. Atmos. 101*(D23), 29641-29652. https://doi.org/10.1029/96JD01866

Mashao, D.C., Kosch, M.J., Bór, J et al., 2021. The altitude of sprites observed over South Africa. *S. Afr. J. Sci. 117*(1-2), 1-8. https://doi.org/10.17159/sajs.2021/7941

McHarg, M.G., Stenbaek- Nielsen, H.C. and Kammae, T., 2007. Observations of streamer formation in sprites. *Geophys. Res. Lett. 34*(6), L06804. https://doi.org/10.1029/2006GL027854

Mlynarczyk, J., Bór, J., Kulak, A et al., 2015. An unusual sequence of sprites followed by a secondary TLE: An analysis of ELF radio measurements and optical observations. *J. Geophys. Res. Space Phys*, *120*(3), 2241-2254. https://doi.org/10.1002/2014ja020780

Neubert, T., Allin, T.H., Blanc, E et al., 2005. Coordinated observations of transient luminous events during the EuroSprite2003 campaign. *J. Atmos. Sol. Terr. Phys. 67*(8-9), pp.807-820. https://doi.org/10.1016/j.jastp.2005.02.004

Neubert, T., Rycroft, M., Farges, T et al., 2008. Recent results from studies of electric discharges in the mesosphere. *Surv. Geophys. 29*(2), 71-137. https://doi.org/10.1007/s10712-008-9043-1

Pasko, V.P., Qin, J. and Celestin, S., 2013. Toward better understanding of sprite streamers: initiation, morphology, and polarity asymmetry. *Surv. Geophys. 34*(6), 797-830. https://doi.org/10.1007/s10712-013-9246-y

Peat, J., Barton, B. and Elliott, E., 2009. Statistics workbook for evidence-based health care. John Wiley & Sons, 93-101. https://doi.org/10.1002/9781444300499

Peng, K.M., Hsu, R.R., Chang, W.Y et al., 2018. Triangulation and coupling of gigantic jets near the lower ionosphere altitudes. *J. Geophys. Res. Space Phys. 123*(8), 6904-6916. https://doi.org/10.1029/2018JA025624

Ren, H., Lu, G., Cummer, S.A et al., 2021. Comparison between high- speed video observation of sprites and broadband sferic measurements. *Geophys. Res. Lett. 48*(10), e2021GL093094. https://doi.org/10.1029/2021GL093094

Rodger, C.J., 1999. Red sprites, upward lightning, and VLF perturbations. *Rev. Geophys. 37*(3), 317-336. https://doi.org/10.1029/1999RG900006

São Sabbas, F.T., Sentman, D.D., Wescott, E.M et al., 2003. Statistical analysis of space–time relationships between sprites and lightning. *J. Atmos. Sol. Terr. Phys. 65*(5), 525-535. https://doi.org/10.1016/S1364-6826(02)00326-7

Sentman, D., Wescott, E., Osborne, D et al., 1995. Preliminary results from the Sprites94 Aircraft Campaign: 1. Red sprites. *Geophys. Res. Lett. 22*(10), 1205-1208. https://doi.org/10.1029/95GL00583

Soula, S., Defer, E., Füllekrug, M et al., 2015. Time and space correlation between sprites and their parent lightning flashes for a thunderstorm observed during the HyMeX campaign. *J. Geophys. Res. Atmos. 120*(22), 11-552. https://doi:10.1002/2015JD023894.

Stenbaek- Nielsen, H.C., Haaland, R., McHarg, M.G et al., 2010. Sprite initiation altitude measured by triangulation. *J. Geophys. Res. Space Phys. 115*(A3), A00E12. https://doi.org/10.1029/2009ja014543

Siingh, D., Singh, R.P., Singh, A.K et al., 2012. Discharges in the stratosphere and mesosphere. *Space sci. rev. 169*(1-4), 73-121. https://doi.org/10.1007/s11214-012-9906-0

Surkov, V.V. and Hayakawa, M., 2020. Progress in the study of transient luminous and atmospheric events: a review. *Surv. Geophys*. *41*, 1101-1142. https://doi.org/10.1007/s10712-020-09597-2

Taylor, M.J., Bailey, M.A., Pautet, P.D et al., 2008. Rare measurements of a sprite with halo event driven by a negative lightning discharge over Argentina. *Geophys. Res. Lett. 35*(14), L14812. https://doi.org/10.1029/2008GL033984

Wang, Y., Lu, G., Ma, M et al., 2019. Triangulation of red sprites observed above a mesoscale convective system in North China. *Earth. Planet. Phys. 3*(2), 111-125. https://doi: 10.26464/epp2019015

Williams, E., Kuo, C.L., Bór, J et al., 2012. Resolution of the sprite polarity paradox: The role of halos. *Radio Sci. 47*(02), 1-12. https://doi.org/10.1029/2011RS004794

Wescott, E.M., Sentman, D.D., Heavner, M.J et al., 1998. Observations of 'Columniform'sprites. *J. Atmos. Sol. Terr. Phys. 60*(7-9), 733-740. https://doi.org/10.1016/s1364-6826(98)00029-7

Wescott, E.M., Stenbaek- Nielsen, H.C., Sentman, D.D et al., 2001. Triangulation of sprites, associated halos and their possible relation to causative lightning and micrometeors. *J. Geophys. Res. Space Phys. 106*(A6), 10467-10477. https://doi.org/10.1029/2000ja000182

Zhu, Y., Rakov, V.A., Tran, M.D et al., 2017. Evaluation of ENTLN performance characteristics based on the ground truth natural and rocket- triggered lightning data acquired

in Florida. *J. Geophys. Res. Atmos. 122*(18), 9858-9866.
https://doi.org/10.1002/2017JD027270

Figure 1

Click here to access/download;Figure;Figure 1.png

Figure 2

Click here to access/download;Figure;Figure 2.png

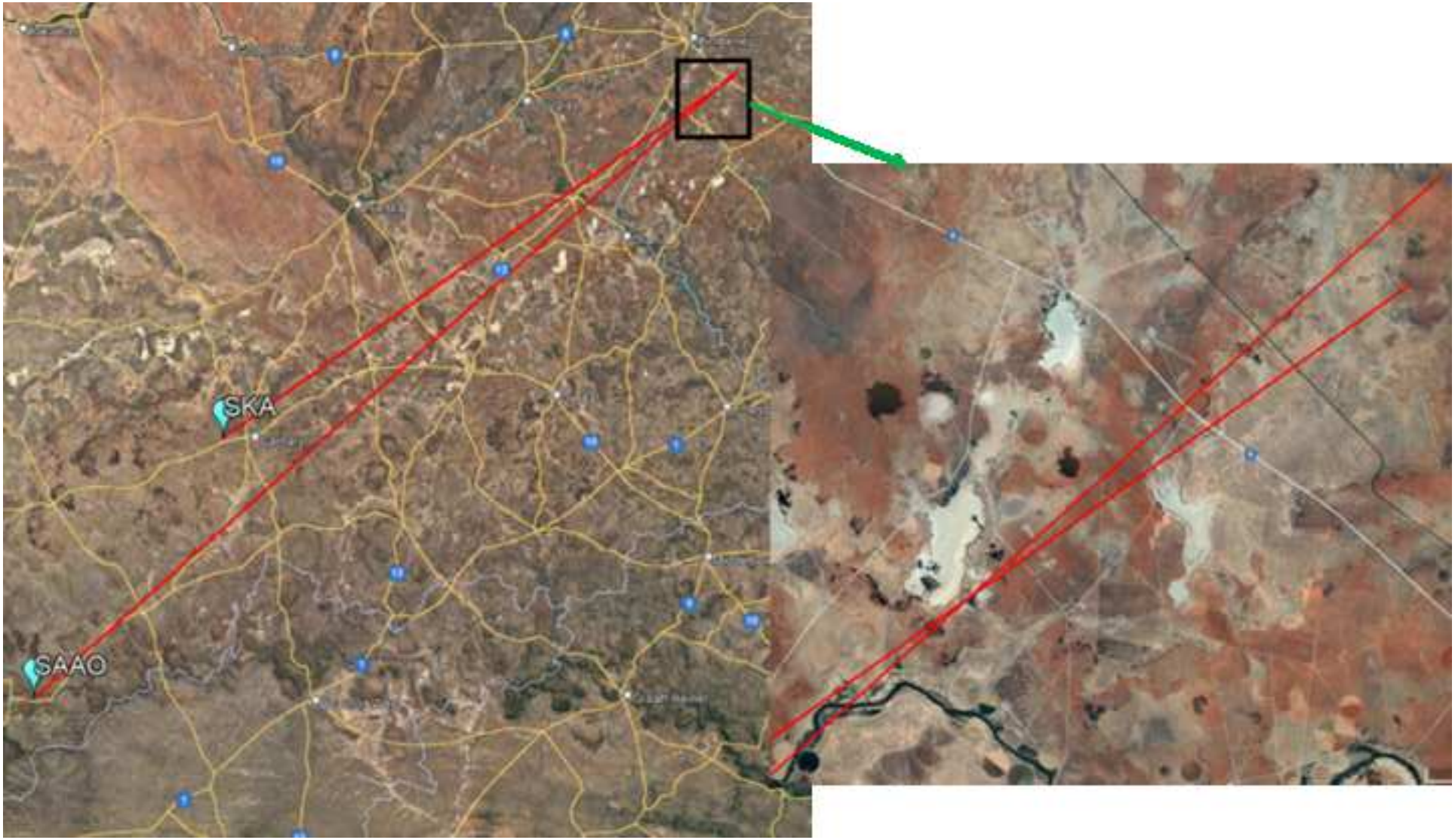

Figure 3

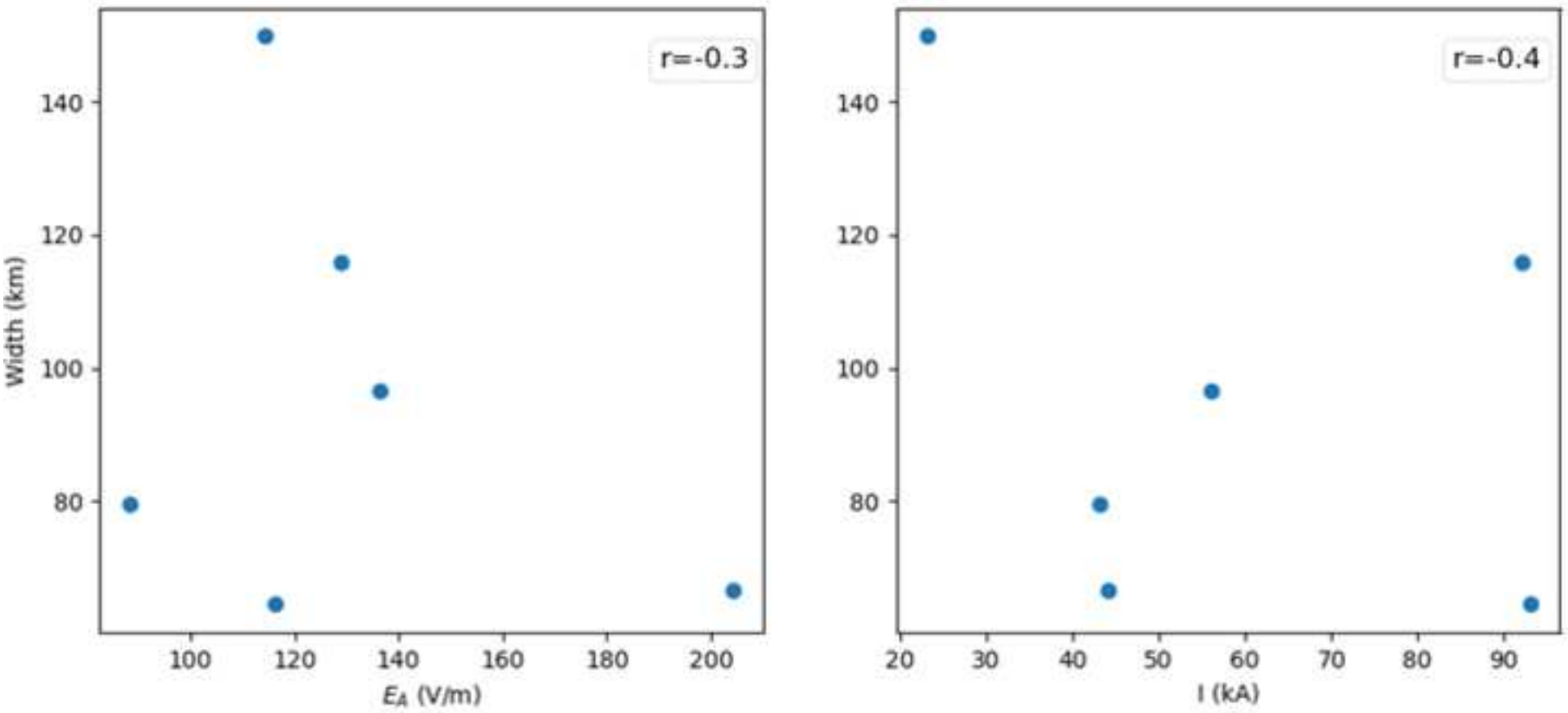

Figure 4

Click here to access/download;Figure;Figure 4.png

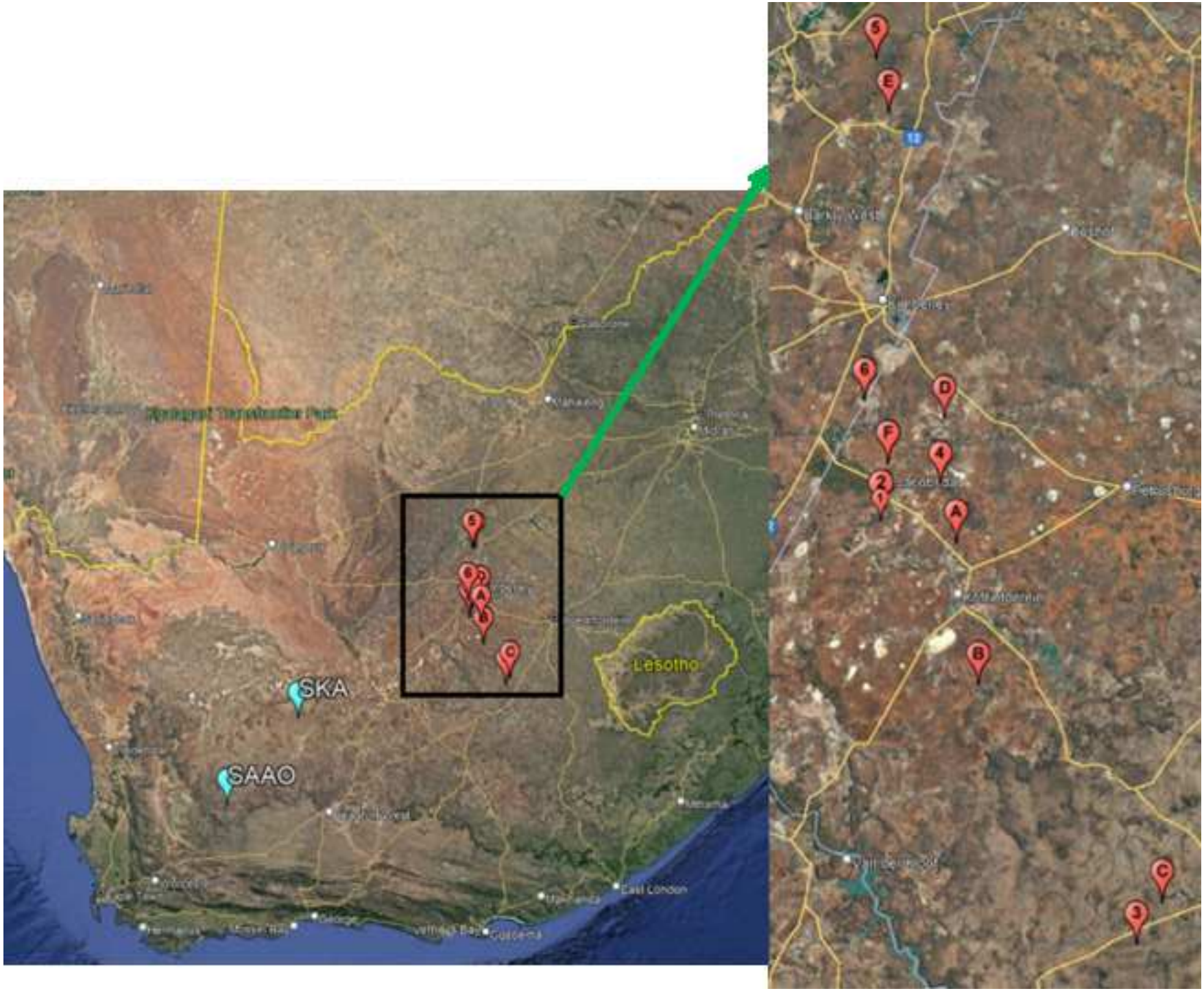

Figure 5

Click here to access/download;Figure;Fugure 5.png

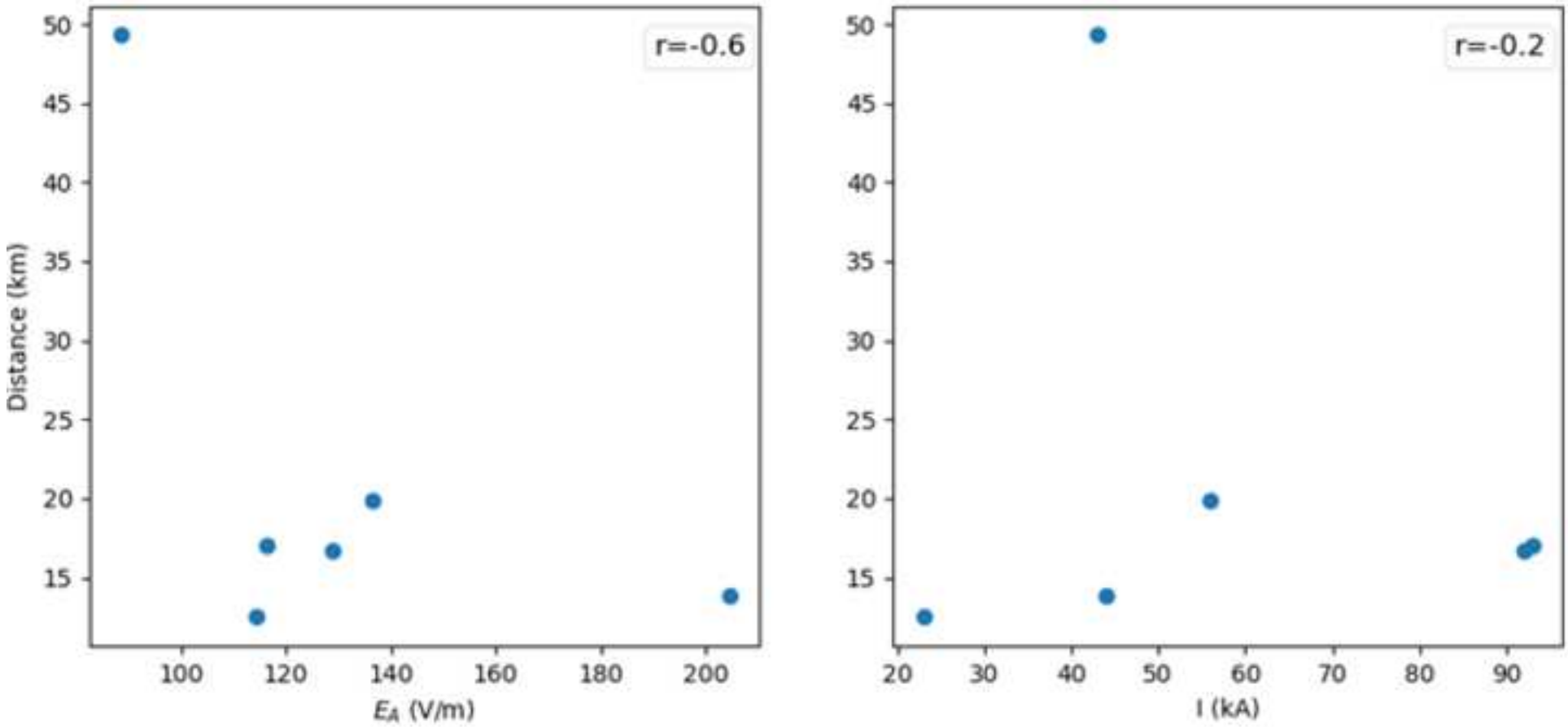

3D triangulation of Transient Luminous Events over Africa

D. Mashao[(1, 2)], M. Kosch[(2,3,4)], M. Fullekrug[(5)], and M. Ivchenko[(6)]

[1]Department of Physics, University of KwaZulu-Natal, Durban 3629, South Africa

[2]South African National Space Agency, Hermanus 7200, South Africa

[3]Department of Physics, Lancaster University, Lancaster LA1 4YB, UK

[4]Department of Physics, University of Western Cape, Bellville 7535, South Africa

[5]Department of Electronic and Electrical Engineering, University of Bath, Bath BA2 7AY, UK

[6]KTH Royal Institute of Technology, Stockholm 114 28, Sweden

Abstract

We present the first 3D triangulation of Transient Luminous Events (TLEs) over Africa. The 6 TLEs were simultaneously observed in the middle atmosphere from Sutherland and Carnarvon in South Africa, separated by 192 km, during the 2019 sprites campaign. These two distinctive locations have low radio interference and are free from light pollution. The lightning times, locations, peak current, and polarities, which initiated the observed TLEs, were obtained from the South African Lightning Detection Network and Earth Networks Total Lightning Networks. We investigate the TLEs' altitude and horizontal displacement from their parent lightning strokes. TLEs appear approximately 12.5 to 49.3 km away from their parent lightning strokes. We found that TLE altitudes range from 29 to 92.6 km. The lightning electric field and peak current may be related to the displacement of TLEs and the TLEs' horizontal spread.

Keywords: Transient Luminous Events triangulation; lightning peak current; lightning electric field.

Corresponding author: Dakalo Mashao (mashaodakalo@gmail.com, +277614725002)

1. Introduction

TLEs such as sprites, elves, blue jets, gigantic jets, starters, and halos, are electrical optical discharge phenomena associated with the lightning activity electric field above thunderstorms at an altitude between about 15 to 100 km above the Earth's surface (Liu et al., 2015; Pasko et al., 2013; Siingh et al., 2012; Surkov and Hayakawa, 2020).

Blue jets, gigantic jets, and starters are connected with intracloud (IC) lightning activity, which involve the positive and negative charges of the thundercloud (Liu et al., 2015; Lu et al., 2011; Peng et al., 2018; Surkov and Hayakawa, 2020). They are generated above the thundercloud and move upwards to an altitude of about 40 to 50 km, 70 to 100 km, and 20 to 30 km, respectively. They have a duration vary from 417 to 650 ms, 60 to 90 ms, and 200 to 300 ms, respectively (Kuo et al., 2015; Liu et al., 2015; Peng et al., 2018; Rodger, 1999; Siingh et al., 2012; Surkov and Hayakawa, 2020).

Elves are a swelling thin ring induced by the electromagnetic pulse of either positive or negative cloud-to-ground (CG) lightning discharge at an altitude of about 85 to 95 km. Elves have a diameter of about 300 to 700 km and a duration of less than 1 ms (Frey et al., 2007; Liu et al., 2015; Williams et al., 2012; Surkov and Hayakawa, 2020). Halos are a spreading diffused flash of light associated with either the positive or negative CG lightning quasi-static electric field at an altitude of about 70 to 90 km (Taylor et al., 2008). Halos have a diameter of about 40 to 89 km and a duration of about 1 ms. Halos are occasionally followed by the initiation of sprites (Frey et al., 2007; Siingh et al., 2012; Surkov and Hayakawa, 2020; Taylor et al., 2008; Williams et al., 2012).

Sprites are very brief optical illuminations about 1 to 10 ms duration in the middle atmosphere at an altitude of about 40 to 90 km, mainly associated with positive CG lightning discharges and sometimes negative CGs (Boggs et al., 2015; Füllekrug et al., 2006; Lang et al., 2013; Liu et al., 2015; Lyons, 1996; Pasko et al., 2013; Siingh et al., 2012; Surkov and Hayakawa, 2020). However, there have been reports of sprites produced by inter or intracloud lightning (Neubert et al., 2005, 2008).

Sprites are the most common form of TLEs. Sprites may appear displaced away from their causal CG lightning locations, e.g. dancing sprites. Most sprites altitude measurements have been done with the assumption that sprites are initiated over their parent lightning strokes, and sprites have been found to occur at an altitude ranging from about 45 to 95 km (Füllekrug et al., 2019; Li et al.,2012; Mashao et al., 2021; McHarg et al., 2007; Ren et al., 2021;

Wescott et al., 1998). There have been reports on sprites altitude triangulation (Sentman et al., 1995; Stenbaek-Nielsen et al., 2010; Soula et al., 2015; Wescott et al., 1998; Wescott et al., 2001), spanning from about 50 to 90 km (Sentman et al., 1995), 48 to 88 km (Wang et al., 2019) and up to 96 km (Stenbaek-Nielsen et al., 2010). Wescott et al. (1998) reported that the column sprites' top altitude ranged from 81.3 to 88.9 km. Wescott et al. (2001) found that triangulation of sprite halos top altitude span from 73.5 to 85.3 km. Factors such as the number of stars visible, local clouds, viewing direction, angular resolution, atmospheric scattering, light pollution, camera gain setting, distance to sprite, and ambiguity in selecting a sprites feature can affect sprites' altitude triangulation (Mlynarczyk et al., 2015).

The displacement between the sprites and their parent lightning strokes ranges from 8.2 to 49.6 km (Wang et al., 2019), 2.4 to 74.7 km (Bór et al., 2018), and 13 to 111 km (Lyons, 1996). Sao-Sabbas et al. (2003) found that most sprites events appeared within 50 km from their parent CG lightning flashes and the maximum displacement was approximately 82 km. According to Lu et al. (2013), sprites are displaced more than 30 km, and according to Mlynarczyk et al. (2015) sprites tend to displace up to 70 km from their parent lightning strokes. Füllekrug et al. (2001) triangulated the lightning current and found a spatial displacement of about 60 km, from the edge of the sprite.

This paper presents the first 3D triangulation of the altitude of TLEs and the horizontal displacement between TLEs and their parent lightning stroke locations observed over Africa. We also compare the lightning electric field strength measured by an extremely low frequency (ELF) receiver and lightning peak current from the lightning networks with the TLEs optical recordings.

2. Observations

On 29 January 2019, 6 TLEs were simultaneously recorded from the South African Astronomical Observatory (SAAO) (32.38º S, 20.81º E) and Square Kilometre Array (SKA) (30.97º S, 21.98º E) in the Northern Cape, South Africa, see Figure 1. The TLEs occurred between 20:49:49 and 22:48:47 UTC. We were able to 3D triangulate the altitude and location of only 6 TLEs due to poor geometry and the aforementioned mitigating factors (Mlynarczyk et al., 2015). Figure 1 shows some of the TLEs observed on 29 January 2019, Gigantic jet (top left) at 20:53:32 UTC, sprites halo (top right) at 20:54:34 UTC, and a column sprites event observed simultaneously at 20:49:49 UTC from SAAO (bottom left) and SKA (bottom right), Northern Cape, South Africa.

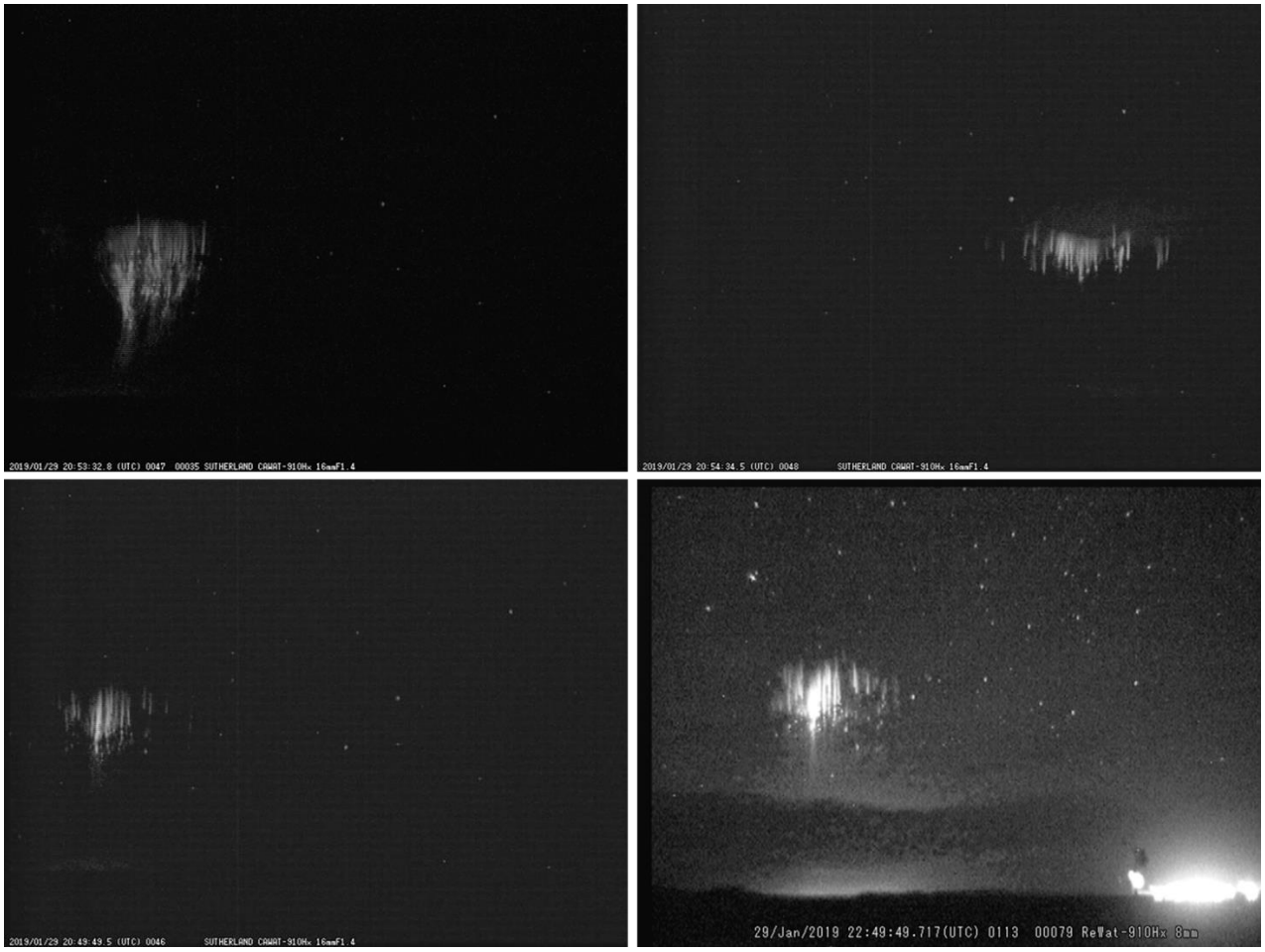

Figure 1. TLEs observed on 29 January 2019. Gigantic jet (top left) and sprites halo (top right) recorded at 20:53:32 and 20:54:34 UTC. Column sprites event observed a 20:49:49 UTC from SAAO (bottom left) and SKA (bottom right), Northern Cape, South Africa.

The triangulated TLEs were recorded using Watec 910Hx cameras with 8.0 mm f/1.4 C-mount lens, which provides a 29°/46.2° Vertical/Horizontal (V/H) Field of View (FOV), see Figure 1. The Watec camera systems captured video frames at 25 fps, 40 ms frame period, 640×480 pixels, fixed gain, and 0.45 gamma factor, with 8-bit intensity resolution and 0.061°/0.072° V/H pixel angular resolution.

2.1 TLEs triangulation

In order to perform successful TLEs altitude and location triangulation, we fitted modeled stars onto the real stars on the background image of TLEs to determine the azimuth and elevation angle of each pixel in the TLE image. Assuming that the TLEs occurred above their parent lightning stoke locations, we estimated the altitude of the target TLE feature, by performing spherical and planar trigonometry in the horizontal plane and vertical planes, respectively. This technique is described in detail by Mashao et al. (2021). After the stars

fitting, we used the cosine and sine rule of spherical trigonometry to obtain simultaneous solutions for the angle subtended on the great circle (A) and slant distance to TLEs (r), as presented in Eq. (1) and (2) below:

$$A = \sin^{-1}\left(\frac{-(2\times(h+R_E)\times(R_E\tan(\theta)))+\sqrt{(2\times(h+R_E)\times R_E\tan(\theta))^2-4\times\left(\frac{(h+R_E)^2}{(\cos(\theta))^2}\right)\times(R_E^2-(h+R_E)^2}}{2\times\left(\frac{(h+R_E)^2}{(\cos(\theta))^2}\right)}\right) \quad (1)$$

$$r = \frac{(h+R_E)\times\sin(A)}{\cos(\theta)} \quad (2)$$

where A is the angle subtended by the great circle, h is the altitude, R_E is the Earth's radius, θ is the elevation angle from the camera locations to the TLEs, and r is the slant distance to the TLEs.

Since we know the azimuth and elevation of every TLEs image pixels and slant distance to the TLEs, for a known altitude, we can convert local spherical coordinates to geographic coordinates to obtain two estimated coordinates (latitude, longitude) of the TLEs with respect to the two observation sites. Since we know the estimated TLEs ground coordinates from each camera's location, we then used Google Earth Pro (version 7.3.4.8248) software to show the distance from the camera systems locations to the TLEs estimated locations, see Figure 2. Figure 2 shows the TLEs position triangulation. The position where the red lines intercept is the actual TLE's location on the ground. We then use the TLE's exact location to adjust the altitude of the TLE by triangulation. By iteration, we resolve the apparent ambiguity between the TLE's geographic position and altitude.

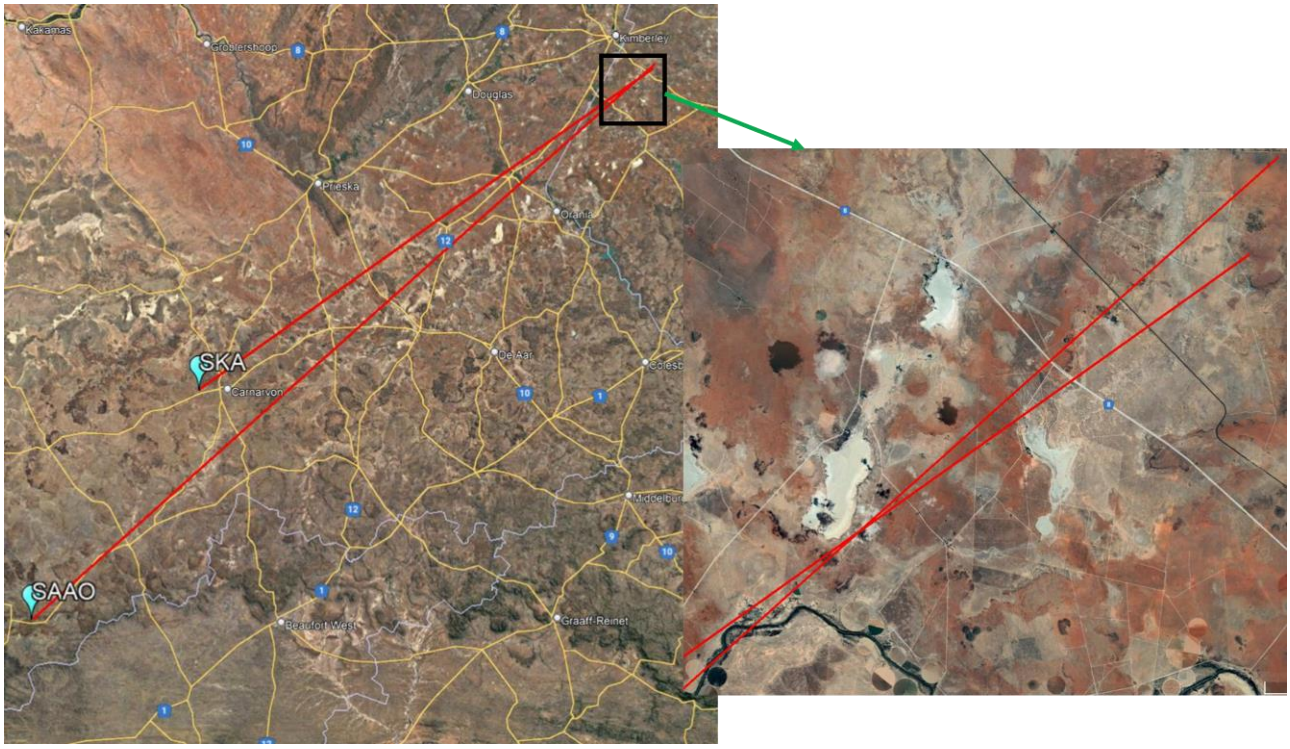

Figure 2. TLE location triangulation. The two turquoise symbols denote the locations of the cameras, which are SAAO and SKA. The red lines mark the distance from the camera locations to the estimated sprite location. The position where the red lines intercept gives the actual TLE's location.

2.2 Lightning detection

The lightning location, time, and peak current information of the causal lightning stroke which generated the TLEs were provided by the South African Lightning Detection Networks (SALDN) and Earth Networks Total Lightning Networks (ENTLN). The SALDN operates 23 sensors with a 90% detection efficiency across South Africa. The SALDN ascertains the lightning locations, occurrence times, and polarities by acquiring the time of arrival and magnetic direction-finding methods. The ENTLN consists of 17 sensors over South Africa with a detection efficiency of approximately 60% to 70%. The ENTLN uses the time of arrival and sophisticated algorithms to determine lightning types, locations, time, and polarities. The SALDN and ENTLN have uncertainties in lightning locations of 0.5 km and 0.2 km, respectively (Gijben, 2012; Zhu et al., 2017). The distance to TLEs from SAAO and SKA were found to span from 511.7 to 590.1 km and 334.0 to 399.7 km, respectively. The parent lightning peak current varied from +9 to +93 kA.

The parent lightning vertical electric fields associated with the TLEs were recorded by a wideband ELF radio receiver, located at SKA, in the frequency range ~4 Hz to 400 kHz. The

ELF radio receiver recorded the lighting vertical electric field with a sampling frequency of 1 MHz and 20 ns time accuracy. The lightning vertical electric field waveforms were used to determine the parent lightning electric field strength and the type of lightning associated with each TLE. The lightning electric field ranged from 204 to 1,570 mV/m at the receiver (Füllekrug, 2010; Füllekrug et al., 2019).

The lightning electric field strength lessens with an increase in distance away from the lightning location. To compensate for this, we determine the electric field amplitude and the attenuation coefficient along the travelled path (Kolmašová et al., 2016). The electric field amplitude coefficient is determined by normalising the maximum lightning electric field strength at the receiver to 100 km from the lightning locations (Kolmašová et al., 2016). We found an experimental attenuation coefficient of about 0.41 dB/100 km. The attenuation of a radio wave signal is low over the nighttime (Chapman and Macario, 1956), and our observations were made at nighttime within a low radio interference area, see Table 1. The attenuation coefficient depends on the bandwidth of the receiver, i.e. low frequency results in low attenuation. Kolmašová et al. (2016) used broadband with a bandwidth of 5 kHz – 37 MHz and obtained an attenuation coefficient of 2.15 dB/100 km (Kolmašová et al., 2016). We found that the electric field amplitude at 100 km from the lightning locations spanned 88.4 to 204 V/m, respectively. All results are summarized in Table 1.

Table 1. Summary of TLEs triangulation observed on the 29 January 2019 as well as their parent lightning occurrence times, positions, and peak current provided by SALDN and ENTLN; lightning vertical electric field recorded by the ELF radio receiver at SKA; distance to sprites from SAAO and SKA; distance between TLE and lightning; TLEs' width and altitude of occurrence; and TLEs' morphological classification. The times in the first column are the lightning occurrence times. +CG and +IC denote positive cloud to ground lightning stroke and positive Intracloud lightning discharge, respectively. The lightning discharge at 20:53:32.904 UTC and 20:53:33.013 UTC contributed to the generation of a gigantic jet. A, B, C, D, E, and F in column 11 (TLEs types) correspond to TLEs position in Figure 4.

Time (UTC)	Lightning location (°)		TLEs location (°)		Distance from SAAO to TLEs (km)	Distance From SKA to TLEs (km)	Lightning peak current (kA)	Electric field at the receiver (mV/m)	Distance between TLE and lightning (km)	TLE maximum Horizontal size (km)	TLEs triangulated Altitude (km)	TLEs types
	LAT	LON	LAT	LON								
20:49:49.668 (+CG)	-29.23	24.79	-29.27	24.99	527.5	345.7	56	1,570	19.9	96.7	39.6—83.3	Column sprites (A)
20:53:32.751 (+CG)	-28.96	24.73	-29.10	24.80	527.6	342	93	1,400	17	64.5	41—89.5	Jellyfish sprites (F)
20:53:32.904 (+CG)	-29.22	24.79	-29.59	25.07	511.7	334.0	43	1,175	49.3	79.7	29—81	Gigantic jet (B)
20:53:33.013 (+IC)	-29.23	24.81	-29.59	25.07			9	204	47.9			
20:54:34.637 (+CG)	-30.19	25.53	-30.06	25.59	522.7	360.3	23	1,101	12.5	149.8	43.3—86.6	Column sprites with (Halo) (C)
21:05:51.251 (+CG)	-29.14	24.94	-28.99	24.94	545.6	360.1	92	1,247	16.7	116	43.5—92.6	Column sprites (D)
22:48:06.932 (+CG)	-28.18	24.71	-28.30	24.75	590.1	399.7	44	1,230	13.9	66.7	47.7—82.6	Column sprites (E)

3. Results and interpretation

3.1 TLEs altitude determination

Six TLEs were triangulated to simultaneously determine the actual TLEs altitude and location. The six TLE events occurred in groups, and most of the TLEs were groups of column sprites. Two TLEs were classified as a jellyfish sprite and a gigantic jet (Surkov and Hayakawa, 2020). The distance from the TLEs to SAAO and SKA varied from 511.7 to 590.1 km and 334 to 399.7 km, respectively. The lightning strokes that initiated the TLEs had a peak current and electric field strength ranging from +23 to +93 kA and 1,101 to 1,570 mV/m at the receiver, respectively. The horizontal size of the 6 TLEs spanned from 64.5 to 149.8 km. The triangulated TLEs altitudes varied from 29 to 92.6 km, see Table 1. One TLE had a halo (see Table 1) of about 132 km diameter.

The TLE, which had a bottom altitude of about 29 km, was classified as a gigantic jet (Surkov and Hayakawa, 2020). The ENTLN reported an IC lightning discharge, which contributed to the initiation of the gigantic jet. The IC lightning discharge occurred 109 ms after the parent +CG lightning stroke and was located 1.7 km from the parent +CG lightning stroke location. The +IC lightning discharge had a peak current and electric field of 9 kA and 204 mV/m at the receiver, respectively. The +IC lightning discharge was 47.9 km away from the gigantic jet. Thus, based on the locations and time of occurrence of the +CG and +IC lightning discharges, both lightning discharges contributed to the initiation of the gigantic jet.

The TLEs' altitude difference between monostatic and triangulated estimates ranged from 1 to 2 km. For the monostatic method, the TLE altitude estimates assumed that TLEs occurred above the causal lightning stroke (Mashao et al., 2021). The uncertainty in TLE altitude determined from the angular resolution of camera varied from ±0.33 to 0.47 km. The uncertainty depends on the slant distance to the TLE from the camera's location, which ranged from 336 to 600 km.

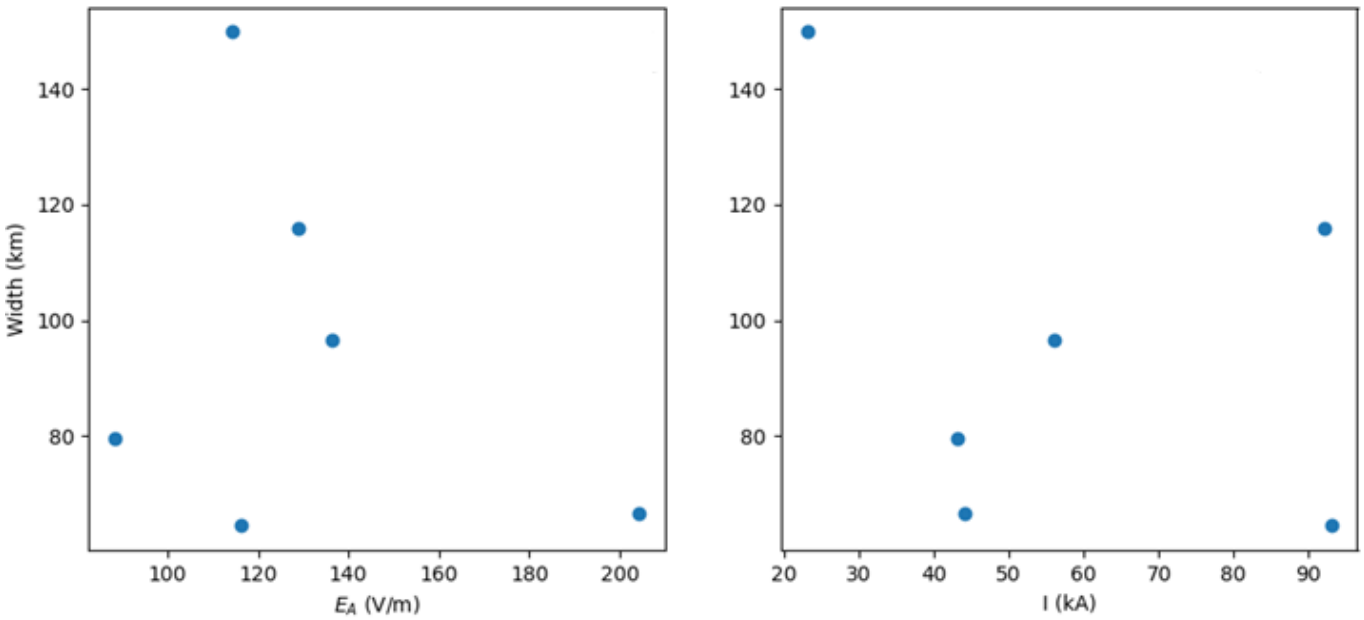

Figure 3. The relationship between the horizontal width of TLEs and the lightning electric field amplitude (E_A) at 100 km from their parent lightning locations (left) and peak current (I) (right), respectively.

Figure 3 shows the relationship between the horizontal width of the TLEs and the lightning electric field amplitude (E_A) (left) at 100 km from their parent lightning locations and peak current (I) (right). The results suggest a decrease in the width of TLEs with an increase in the lightning electric field amplitude and peak current, respectively, although the data set is small and the spread too large to draw a clear conclusion.

3.2 TLEs position triangulation

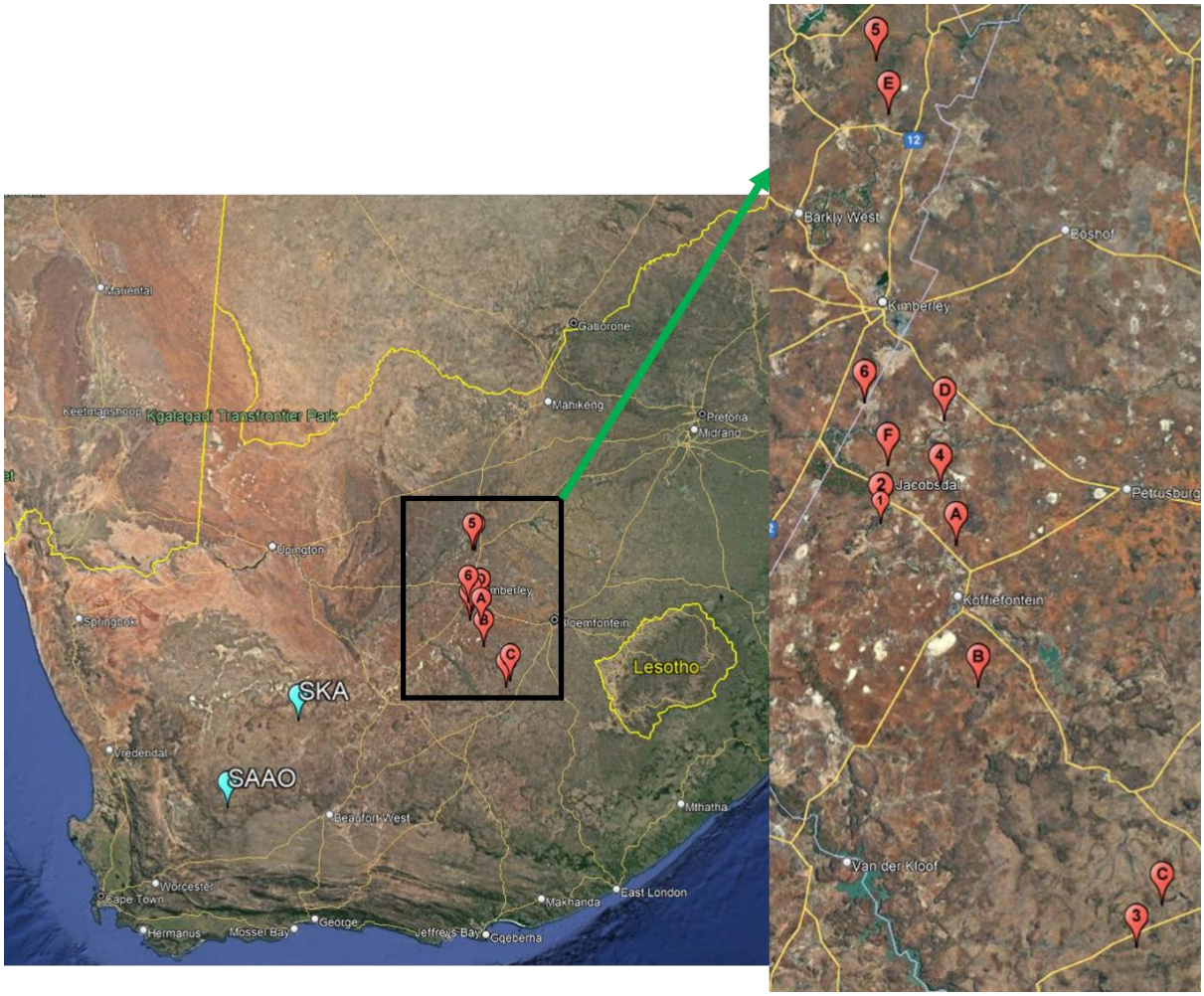

Figure 4. The locations of TLEs and their parent lightning strokes. The numbers and letters correspond to the position of parent lightning strokes and TLEs, respectively. E.g., lightning stroke 1, 2, 3, 4, 5, and 6 corresponds to TLE A, B, C, D, E, and F. SKA and SAAO mark the positions of the cameras.

The displacement between 6 triangulated TLE features and their parent lightning stroke position were from 12.5 to 49.3 km. Our results are in good agreement with similar results obtained elsewhere (Bór et al., 2018; Lu et al., 2013; Lyons, 1996; Mlynarczyk et al., 2015; Sao-Sabbas et al., 2003; Wang et al., 2019). The uncertainty in sprites geographic location, which depends on the angular resolution of the cameras and the viewing geometry to the TLEs, averaged 7.2 km with a standard deviation of 7.1 km. Figure 4 shows the TLEs' displacement from their parent lightning strokes.

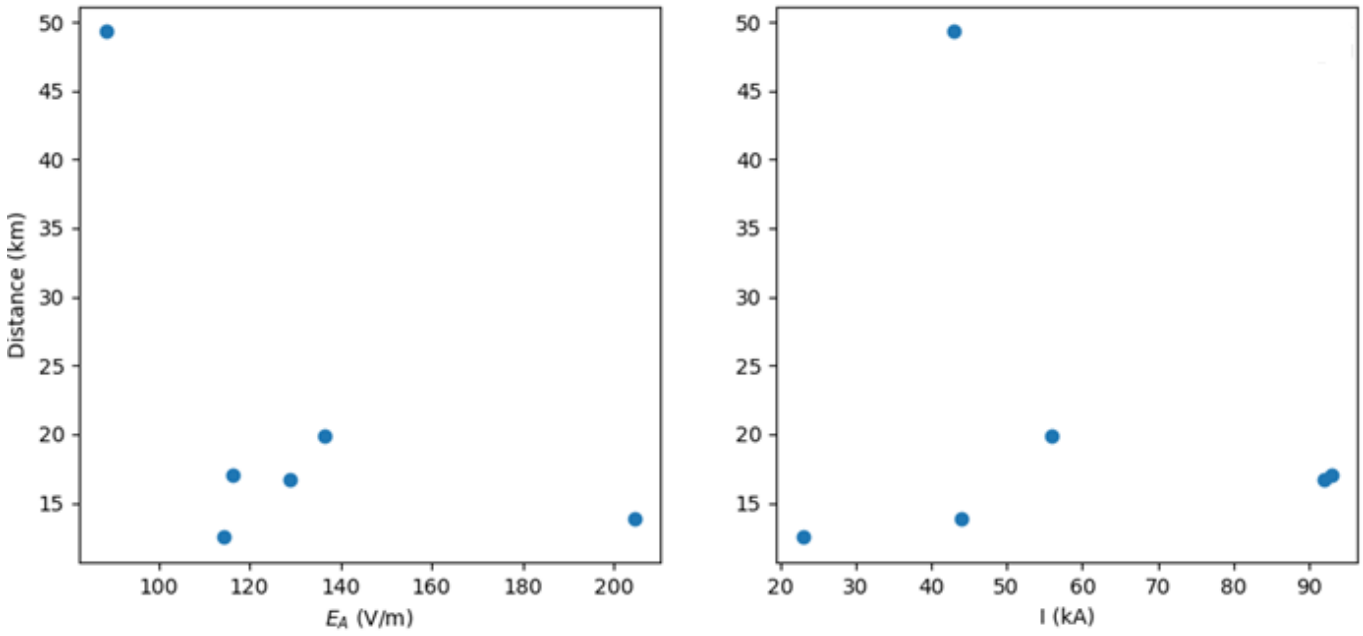

Figure 5. TLEs displayed distance from their parent lightning versus lightning electric field amplitude (E_A) at 100 km from their lightning locations (left) and peak current (I) (right), respectively.

The relationship between the TLEs' displaced distance from their parent lightning and the lightning electric field amplitude (E_A) and peak current (I) is shown in Figure 5. The TLEs displacement distance may decrease with an increase in the lightning electric field amplitude and peak current, respectively, although again the data set is small and the spread too large to draw a clear conclusion. A large parent lightning electric field makes it more likely that the atmosphere overhead exhibits dielectric breakdown. Therefore, lightning discharges with large electric fields result in a small TLE displacement away from their parent lightning stroke. We note the poor statistics.

Summary and Conclusions

We present the 3D triangulation of six TLEs positions on the Earth's surface and atmospheric altitudes. The CG lightning discharges associated with the TLEs have peak currents varying from +23 to +93 kA. The CG lightning electric field strength at the receiver and normalised to 100 km from their lightning stroke locations vary from 1,101 to 1,570 mV/m and 88.4 to 204 V/m, respectively. We found that the TLE displacement away from the lightning location spanned from 12.5 to 49.3 km. The triangulated altitudes of the TLEs ranged from 29 to 92.6 km, and their width varied from 64.5 to 149.8 km. The TLEs displacement away from their parent lightning and TLE width may decrease with an increase in their parent lightning normalised electric field amplitude. However, more data is required to confirm these results.

The TLEs initiated by parent lightning with a large electric field strength and peak current tend to display near their parent lightning location and with a less horizontal width.

4. Acknowledgments

This work was sponsored by the South African National Space Agency, University of KwaZulu-Natal, and the Royal Society (UK) grant NMG/R1/180252. DM, KM, and MF thank the sponsors for their support. The authors thank the South African Lightning Detection Networks and Earth Networks Total Lightning Networks for providing the lightning data.

5. References:

Boggs, L.D, Liu, N., Splitt, M et al., 2016. An analysis of five negative sprite- parent discharges and their associated thunderstorm charge structures. *J. Geophys. Res. Atmos*. *121*(2), 759-784. https://doi.org/10.1002/2015JD024188

Bór, J., Zelkó, Z., Hegedüs, T et al., 2018. On the series of+ CG lightning strokes in dancing sprite events. *J. Geophys. Res. Atmos*. *123*(19), 11-030. https://doi.org/10.1029/2017JD028251

Chapman, F.W. and Macario, R.C.V., 1956. Propagation of audio-frequency radio waves to great distances. *Nature, 177*(4516), 930-933. https://doi.org/10.1038/177930a0

Frey, H.U., Mende, S.B., Cummer, S.A., et al., 2007. Halos generated by negative cloud-to- ground lightning. *Geophys. Res. Lett*. 34(18), L18801. https://doi.org/10.1029/2007gl030908

Füllekrug, M., Moudry, D.R., Dawes, G et al., 2001. Mesospheric sprite current triangulation. *J. Geophys. Res. Atmos. 106*(D17), 20189-20194. https://doi.org/10.1029/2001JD900075

Füllekrug, M., Mareev, E.A. Rycroft, M.J. eds., 2006. Sprites, Elves and intense Lightning Discharges (Vol. 225). *NATO Science Series II. Mathematics, physics and chemistry*, Dordrecht: *Springer*, ISBN 1-4020-4628-630-42, 30-32. https://doi.org/10.1007/1-4020-4629-4

Füllekrug, M., 2010. Wideband digital low-frequency radio receiver. *Meas. Sci. Technol. 21*(1), 1-9. https://doi.org/10.1088/0957-0233/21/1/015901

Füllekrug, M., Nnadih, S., Soula, S et al., 2019. Maximum sprite streamer luminosity near the Stratopause. *Geophys. Res. Lett*. *46*(21), 12572-12579. https://doi.org/10.1029/2019GL084331

Gijben, M., 2012. The lightning climatology of South Africa. *S. Afr. J. Sci*, *108*(3), 1-10. https://doi.org/10.4102/sajs.v108i3/4.740

Kolmašová, I., Santolík, O., Farges, T et al., 2016. Subionospheric propagation and peak currents of preliminary breakdown pulses before negative cloud- to- ground lightning discharges. *Geophys. Res. Lett. 43*(3), 1382-1391. https://doi:10.1002/2015GL067364.

Kuo, C.L., Su, H.T. and Hsu, R.R., 2015. The blue luminous events observed by ISUAL payload on board FORMOSAT- 2 satellite. *J. Geophys. Res. Space Phys. 120*(11), 9795-9804. https://doi.org/10.1002/2015JA021386

Lang, T.J., Cummer, S.A., Rutledge, S.A et al., 2013. The meteorology of negative cloud-to- ground lightning strokes with large charge moment changes: Implications for negative sprites. *J. Geophys. Res. Atmos. 118*(14), 7886-7896. https://doi.org/10.1002/jgrd.50595

Li, J., Cummer, S., Lu, G. et al., 2012. Charge moment change and lightning- driven electric fields associated with negative sprites and halos. *J. Geophys. Res. Space Phys*. *117*(A9), A09310. https://doi.org/10.1029/2012JA017731

Liu, N., McHarg, M.G. and Stenbaek-Nielsen, H.C., 2015. High-altitude electrical discharges associated with thunderstorms and lightning. *J. Atmos. Sol. Terr. Phys. 136*, 98-118. https://doi.org/10.1016/j.jastp.2015.05.013

Lu, G., Cummer, S.A., Lyons, W.A et al., 2011. Lightning development associated with two negative gigantic jets. *Geophy. Res. Lett. 38*(12), L12801. https://doi.org/10.1029/2011GL047662

Lu, G., Cummer, S.A., Li, J et al., 2013. Coordinated observations of sprites and in- cloud lightning flash structure. *J. Geophys. Res. Atmos. 118*(12), 6607-6632. https://doi.org/10.1002/jgrd.50459

Lyons, W.A., 1996. Sprite observations above the US High Plains in relation to their parent thunderstorm systems. *J. Geophys. Res. Atmos. 101*(D23), 29641-29652. https://doi.org/10.1029/96JD01866

Mashao, D.C., Kosch, M.J., Bór, J et al., 2021. The altitude of sprites observed over South Africa. *S. Afr. J. Sci. 117*(1-2), 1-8. https://doi.org/10.17159/sajs.2021/7941

McHarg, M.G., Stenbaek- Nielsen, H.C. and Kammae, T., 2007. Observations of streamer formation in sprites. *Geophys. Res. Lett. 34*(6), L06804. https://doi.org/10.1029/2006GL027854

Mlynarczyk, J., Bór, J., Kulak, A et al., 2015. An unusual sequence of sprites followed by a secondary TLE: An analysis of ELF radio measurements and optical observations. *J. Geophys. Res. Space Phys*, *120*(3), 2241-2254. https://doi.org/10.1002/2014ja020780

Neubert, T., Allin, T.H., Blanc, E et al., 2005. Coordinated observations of transient luminous events during the EuroSprite2003 campaign. *J. Atmos. Sol. Terr. Phys. 67*(8-9), pp.807-820. https://doi.org/10.1016/j.jastp.2005.02.004

Neubert, T., Rycroft, M., Farges, T et al., 2008. Recent results from studies of electric discharges in the mesosphere. *Surv. Geophys. 29*(2), 71-137. https://doi.org/10.1007/s10712-008-9043-1

Pasko, V.P., Qin, J. and Celestin, S., 2013. Toward better understanding of sprite streamers: initiation, morphology, and polarity asymmetry. *Surv. Geophys. 34*(6), 797-830. https://doi.org/10.1007/s10712-013-9246-y

Peng, K.M., Hsu, R.R., Chang, W.Y et al., 2018. Triangulation and coupling of gigantic jets near the lower ionosphere altitudes. *J. Geophys. Res. Space Phys. 123*(8), 6904-6916. https://doi.org/10.1029/2018JA025624

Ren, H., Lu, G., Cummer, S.A et al., 2021. Comparison between high- speed video observation of sprites and broadband sferic measurements. *Geophys. Res. Lett. 48*(10), e2021GL093094. https://doi.org/10.1029/2021GL093094

Rodger, C.J., 1999. Red sprites, upward lightning, and VLF perturbations. *Rev. Geophys. 37*(3), 317-336. https://doi.org/10.1029/1999RG900006

São Sabbas, F.T., Sentman, D.D., Wescott, E.M et al., 2003. Statistical analysis of space–time relationships between sprites and lightning. *J. Atmos. Sol. Terr. Phys. 65*(5), 525-535. https://doi.org/10.1016/S1364-6826(02)00326-7

Sentman, D., Wescott, E., Osborne, D et al., 1995. Preliminary results from the Sprites94 Aircraft Campaign: 1. Red sprites. *Geophys. Res. Lett. 22*(10), 1205-1208. https://doi.org/10.1029/95GL00583

Soula, S., Defer, E., Füllekrug, M et al., 2015. Time and space correlation between sprites and their parent lightning flashes for a thunderstorm observed during the HyMeX campaign. *J. Geophys. Res. Atmos. 120*(22), 11-552. https://doi:10.1002/2015JD023894.

Stenbaek- Nielsen, H.C., Haaland, R., McHarg, M.G et al., 2010. Sprite initiation altitude measured by triangulation. *J. Geophys. Res. Space Phys. 115*(A3), A00E12. https://doi.org/10.1029/2009ja014543

Siingh, D., Singh, R.P., Singh, A.K et al., 2012. Discharges in the stratosphere and mesosphere. *Space sci. rev. 169*(1-4), 73-121. https://doi.org/10.1007/s11214-012-9906-0

Surkov, V.V. and Hayakawa, M., 2020. Progress in the study of transient luminous and atmospheric events: a review. *Surv. Geophys. 41,* 1101-1142. https://doi.org/10.1007/s10712-020-09597-2

Taylor, M.J., Bailey, M.A., Pautet, P.D et al., 2008. Rare measurements of a sprite with halo event driven by a negative lightning discharge over Argentina. *Geophys. Res. Lett. 35*(14), L14812. https://doi.org/10.1029/2008GL033984

Wang, Y., Lu, G., Ma, M et al., 2019. Triangulation of red sprites observed above a mesoscale convective system in North China. *Earth. Planet. Phys. 3*(2), 111-125. https://doi: 10.26464/epp2019015

Wescott, E.M., Sentman, D.D., Heavner, M.J et al., 1998. Observations of 'Columniform'sprites. *J. Atmos. Sol. Terr. Phys. 60*(7-9), 733-740. https://doi.org/10.1016/s1364-6826(98)00029-7

Wescott, E.M., Stenbaek- Nielsen, H.C., Sentman, D.D et al., 2001. Triangulation of sprites, associated halos and their possible relation to causative lightning and micrometeors. *J. Geophys. Res. Space Phys. 106*(A6), 10467-10477. https://doi.org/10.1029/2000ja000182

Williams, E., Kuo, C.L., Bór, J et al., 2012. Resolution of the sprite polarity paradox: The role of halos. *Radio Sci. 47*(02), 1-12. https://doi.org/10.1029/2011RS004794

Zhu, Y., Rakov, V.A., Tran, M.D et al., 2017. Evaluation of ENTLN performance characteristics based on the ground truth natural and rocket- triggered lightning data acquired in Florida. *J. Geophys. Res. Atmos. 122*(18), 9858-9866. https://doi.org/10.1002/2017JD027270

To the Reviewers,

Thank you so much for the fruitful response. We have revised the manuscript accordingly. Please see our comments and responses below in green. The voluntary changes (new paragraphs and whole new sentences) are written in green text in the manuscript.

Reviewer #1: .

Reviewer #2: The revised manuscript has been improved. However, I believe that the authors have not sufficiently addressed my previous comment (c). (See attachment.) They have removed the linear regression lines from Figures 3 and 5, but they do not properly discuss the fact that the linear regression coefficients and the stated/suggested relationships between the variables in these figures are strongly influenced by some unusually large values (outliers). I strongly recommend discussing this.

We have removed the linear regression coefficients in figures 3 and 5, since the relationships between the variables in the figures are influenced significantly by some outliers. The discussion regarding this has been added in the manuscript on page 10, lines 220-222, and on page 12, lines 239-242.

-Another comment related to the new text on lines 203-204, "…after the +CG lightning stroke located 1.7 km away from the +CG lightning stroke location." makes no sense for me. Please reformulate

The text has been reformed in the manuscript on page 9, lines 202-205.

Thank you